

# MORIME: A multi-objective RIME optimization framework for efficient truss design

Mohammad Aljaidi <sup>a</sup>, Nikunj Mashru <sup>b</sup>, Pinank Patel <sup>b</sup>, Divya Adalja <sup>c</sup>, Pradeep Jangir <sup>d,e,f</sup>, Arpita <sup>g</sup>, Sundaram B. Pandya <sup>h</sup>, Mohammad Khishe <sup>i,j,\*</sup>

<sup>a</sup> Department of Computer Science, Faculty of Information Technology, Zarqa University, Zarqa 13110, Jordan

<sup>b</sup> Department of Mechanical Engineering, Marwadi University, Rajkot, 360003, India

<sup>c</sup> Department of Mathematics, Marwadi University, Rajkot, 3630003, India

<sup>d</sup> Adjunct Professor, Department of CSE, Graphic Era Hill University, Dehradun, 248002, India

<sup>e</sup> Adjunct Professor, Department of CSE, Graphic Era Deemed To Be University, Dehradun, 248002, Uttarakhand, India

<sup>f</sup> Applied Science Research Center, Applied Science Private University, Amman 11931, Jordan

<sup>g</sup> Department of Biosciences, Saveetha School of Engineering, Saveetha Institute of Medical and Technical Sciences, Chennai, 602105 India

<sup>h</sup> Department of Electrical Engineering, Shri K.J. Polytechnic, Bharuch 392001, India

<sup>i</sup> Department of Electrical Engineering, Imam Khomeini Naval Science University of Nowshahr, Nowshahr, Iran

<sup>j</sup> Jadara University Research Center, Jadara University, Irbid, Jordan

## ARTICLE INFO

### Keywords:

Structural engineering  
Pareto optimality  
Compliance reduction  
Multiobjective optimization

## ABSTRACT

Multi objective optimization (MOO) is very important in structural engineering, especially in truss design where a trade off between weight reduction and compliance is needed to maximize the efficiency. Usually, conventional optimization algorithms have difficulty in solving complex MOO tasks, and in generating diverse, high quality solutions for various structural configurations. To overcome these challenges, this study proposes a Multi Objective RIME (MORIME) algorithm that uses improved non-dominated sorting and crowding distance techniques to optimize weight and compliance over eight truss designs. With respect to Hypervolume (HV), Inverted Generational Distance (IGD), and Spacing (SP) metrics, it performed better than other established methods such as NSGA-II, MOEA/D, MOMVO, MOTEQ, MOLCA, and MORIME, leading to better convergence and diversity of solution sets. The results show that MORIME is a good tool for dealing with complex multi objective optimization landscapes and that it is better than biologically inspired and hybrid optimization methods. MORIME is a powerful tool for structural engineers to produce well balanced truss designs, which meet stringent weight and compliance requirements in a multiobjective setting. MORIME is one attractive feature because it can generate optimal and diverse solutions in truss optimization, resulting in high quality design results.

## 1. Introduction

Over the past few years, metaheuristic algorithms have become indispensable in solving complex optimization problems in wide engineering and scientific fields. In contrast to traditional methods, metaheuristics are flexible and adaptable, using ideas from nature, such as biological evolution, social behavior and physics [1]. In large-scale, complex problem spaces, they are particularly effective where conventional optimization techniques fail [2]. Genetic Algorithm (GA) [3], Particle Swarm Optimization (PSO) [4], and Ant Colony Optimization (ACO) [5], are classic metaheuristic algorithms that have been widely

applied in areas such as structural engineering and machine learning. They offer a robust framework for balancing exploration and exploitation in the search space and, hence, are very useful for solving complex real-world problems [6,7].

The backbone of problem-solving in engineering is optimization techniques, as one usually tries to improve systems for efficiency, cost-effectiveness, or performance. Generally, the optimization can be classified as single-objective and multi-objective optimization. In contrast to differential methods applied by traditional optimization, modern techniques operate with heuristic and metaheuristic, or with the use of heuristic and metaheuristic, when solving nonlinear problems. Material

\* Corresponding author.

E-mail addresses: [mjaidi@zu.edu.jo](mailto:mjaidi@zu.edu.jo) (M. Aljaidi), [nikunj.mashru039@gmail.com](mailto:nikunj.mashru039@gmail.com) (N. Mashru), [pinankpatel19@gmail.com](mailto:pinankpatel19@gmail.com) (P. Patel), [pateldivya91@gmail.com](mailto:pateldivya91@gmail.com) (D. Adalja), [pkjmttech@gmail.com](mailto:pkjmttech@gmail.com) (P. Jangir), [apyjangid@gmail.com](mailto:apyjangid@gmail.com) (Arpita), [sundarampandya@gmail.com](mailto:sundarampandya@gmail.com) (S.B. Pandya), [m\\_khishe@alumni.iust.ac.ir](mailto:m_khishe@alumni.iust.ac.ir) (M. Khishe).

<https://doi.org/10.1016/j.rineng.2025.103933>

Received 18 November 2024; Received in revised form 21 December 2024; Accepted 1 January 2025

Available online 2 January 2025

2590-1230/© 2025 The Author(s). Published by Elsevier B.V. This is an open access article under the CC BY license (<http://creativecommons.org/licenses/by/4.0/>).

science, robotics, and other structural design advances have been achieved by integrating these techniques with computational power. As engineering systems become more complex, the critical need to refine and advance optimization algorithms arises, since simple performance improvements can translate to large practical benefits.

Single-objective optimization (SOO) focuses on improving a solitary criterion, such as minimizing cost or maximizing efficiency. This approach, while straightforward, often encounters limitations in multi-dimensional design spaces where real-world problems typically require consideration of multiple, frequently conflicting objectives. SOO methods have been foundational in many optimization studies, especially in fields with a dominant goal. Techniques like linear programming, quadratic programming, and metaheuristic-based single-objective optimizers have been extensively explored. However, the single-objective framework falls short when balancing multiple trade-offs, making multi-objective optimization essential in complex scenarios. Recently proposed SOO techniques, i.e., Remora optimization algorithm, [8], Run beyond the metaphor [9], snow ablation optimizer [10], white shark optimizer [11], Newton-Raphson-based optimizer [12], Sled dog optimizer [13], Polar Light Optimizer [14], Resistance-capacitance optimizer [15], Parrot Optimizer [16], are very powerful in finding optimum solutions.

Multi-objective optimization (MOO) addresses this limitation by aiming to simultaneously optimize two or more objectives. In structural engineering, for example, weight reduction and compliance minimization are often conflicting yet critical goals. Multi-objective metaheuristics, such as NSGA-II [17], MOEA/D [18], and MOGMO [19], MOMVO [20], MOHO [21], MOSAO [22], MORCA [23], MOEO [24], MOLCA [25], MOEDO [26], MOWSA [27], are designed to navigate these competing objectives by generating diverse Pareto-optimal solutions, offering trade-offs between objectives. MOO allows decision-makers to choose the most suitable solution based on contextual priorities. Despite its advantages, MOO remains computationally challenging due to the need for diverse, high-quality solutions representing a balanced trade-off between objectives.

As established by optimization theory informed by the 'No Free Lunch' (NFL) theorem [28] of Wolpert and Macready, there is no optimization algorithm that performs better than all other algorithms in all problem domains. This theorem emphasizes that picking or design a problem-specific optimization algorithm is as crucial as to make it effective in terms of performance. In the case of truss structure optimization, it is clear that no metaheuristic is universally better than the others and therefore there is a never ending search for new algorithms or hybrid approaches that will perform better. Optimization problems, as evidenced by the NFL theorem, present a strong case for the exploration of new methodologies, including the Multi-Objective RIME (MORIME) algorithm [29] presented in this study.

Optimization of truss structure is an important field of structural engineering, where the aim is usually to minimize weight and maximize structural compliance and integrity [30]. Truss designs that are efficient are necessary for minimizing material use, reducing costs, and increasing load bearing capacity. However, traditional optimization methods have difficulty dealing with the complex, multi objective nature of truss design, as they are not robust enough to traverse high dimensional and non linear design spaces. Therefore, metaheuristic based MO optimization techniques have become popular for truss structure design in order to design lightweight yet durable structures. In this study, the MORIME algorithm proposed addresses these challenges by using advanced non-dominated sorting and crowding distance methods, providing an efficient solution to multi-objective truss optimization.

### 1.1. Contributions

- Development of the MORIME algorithm for multi-objective truss structure optimization.

- Apply MORIME to optimize truss weight and compliance across eight configurations, advancing existing methodologies.
- Comparative evaluation of MORIME against leading algorithms (NSGA-II, MOEA/D, MOMVO, MOTEQ, MOLCA), demonstrating superior performance in Hypervolume, Inverted Generational Distance, and Spacing metrics.
- Provision of a new framework for structural engineers to achieve efficient, high-quality truss designs, mainly where multiple objectives constrain decision-making.

In this paper, we present an innovative truss optimization approach that is more efficient and has a greater solution diversity than traditional methods. In the following section, we discuss the mathematical framework of MORIME, including the design of the algorithm and its distinctive features.

The following contributions were made to this study:

- In [Section 2](#), the mathematical framework of the MORIME algorithm is presented, with the emphasis on its improved non-dominated sorting and crowding distance strategies. These elements are intended to enhance solution diversity and convergence, which are necessary for efficient multi objective optimization in structural engineering.
- In [Section 3](#), the truss optimization problem is defined, with the dual objectives of weight and compliance minimization as the key to efficient structural designs. In this section, we discuss how MORIME specifically deals with these objectives within a multi objective optimization context, optimizing truss performance for different configurations.
- In [Section 4](#), the evaluation metrics used in the study are outlined: Hypervolume (HV), Inverted Generational Distance (IGD), Spacing, and computational Run Time. Together, these metrics measure MORIME ability to produce an optimal and well distributed Pareto front, and confirm its effectiveness in complex optimization problems.
- Experimental evaluation of MORIME is presented in [Section 5](#), along with a comparative analysis with other established algorithms including NSGA-II, MOEA/D, MOMVO, MOLCA and MOTEQ. In this section, MORIME performance across various truss configurations is demonstrated using detailed performance metrics and statistical comparisons to demonstrate its ability to solve complex MO problems.
- Finally, [Section 6](#) concludes the study and summarizes the main findings, discusses the potential application of MORIME in multi-objective structural optimization and suggests future research directions to further extend its applicability.

This structure presents a complete picture of MORIME development, application, and evaluation, as well as its contributions to truss structure optimization.

## 2. Theoretical foundation and mathematical modeling of MORIME

A powerful optimization tool for solving complex multi objective problems, especially when a balance of conflicting objectives is needed, such as in structural engineering, is the Multi Objective RIME (MORIME) algorithm. MORIME combines advanced non-dominated sorting and crowding distance calculations with mechanisms inspired by rime ice formation to produce a diverse and high quality Pareto front. MORIME is capable of handling non-linear high dimensional problems through its structured approach, and provides a systematic approach to exploration and convergence. MORIME is a versatile solution for multi-objective optimization tasks, providing engineers and researchers an effective solution to generate optimal designs across competing objectives within a mathematical framework.

## 2.1. Population initialization

In the MORIME algorithm, the initial population forms the starting point for optimization, setting the stage for iterative solution space exploration.

Each individual in the population represents a potential solution, denoted as a vector  $X_i$  of  $D$  dimensions (decision variables). For a population of  $N$  individuals, each dimension  $j$  is initialized as:  $X_{i,j} = LB_j + \text{rand}(0, 1) \times (UB_j - LB_j)$  where:  $LB_j$  and  $UB_j$  are the lower and upper bounds of the  $j^{\text{th}}$  variable, respectively.  $\text{rand}(0, 1)$  is a random number between 0 and 1, ensuring that each solution vector is randomly spread across the feasible solution space. This randomized initialization promotes diversity in the starting population, enhancing the algorithm ability to explore the entire solution space and avoid early convergence on local optima.

## 2.2. Non-Dominated sorting

Non-dominated sorting organizes the population into Pareto fronts, which is essential for multi-objective optimization where multiple objectives may conflict.

### 2.2.1. Dominance criteria

In the dominance criteria for multi-objective optimization, let  $M$  denote the number of objective functions to be optimized. A solution  $p$  is said to dominate another solution  $q$  if and only if the following conditions are satisfied:  $f_k(p) \leq f_k(q)$  for all  $k \in \{1, 2, \dots, M\}$ , and there exists at least one objective  $j \in \{1, 2, \dots, M\}$  such that  $f_j(p) < f_j(q)$ . This means that solution  $p$  is at least as good as solution  $q$  in all objectives and strictly better in at least one objective.

**Front Formation:** Non-dominated sorting divides the population into layers of non-dominated fronts  $F_1, F_2, \dots, F_l$ : The first front  $F_1$  contains solutions that are not dominated by any other solutions in the population. The second front  $F_2$  consists of solutions that are only dominated by those in  $F_1$ , and so on. Organizing solutions into fronts allows MORIME to prioritize non-dominated solutions and ensure distribution across the solution space, which is crucial for maintaining diversity in multi-objective optimization.

## 2.3. Crowding distance calculation

Crowding distance quantifies the diversity within each Pareto front by measuring the ‘‘crowdedness’’ around each solution.

For a given solution  $i$  in a front, the crowding distance  $d_i$  is calculated as per Eq. (1).

$$d_i = d_i + \sum_{m=1}^M \frac{f_{m,i+1} - f_{m,i-1}}{f_m^{\max} - f_m^{\min}} \quad (1)$$

Where:  $f_{m,i+1}$  and  $f_{m,i-1}$  are the objective values of neighbouring solutions in objective  $m$ ,  $f_m^{\max}$  and  $f_m^{\min}$  represent the maximum and minimum values of objective  $m$  in the current front. To preserve boundary diversity, boundary solutions in each front are assigned an infinite crowding distance. Crowding distance ensures that selected solutions are well spread across the Pareto front. Solutions in less crowded regions are favoured, preserving diversity and helping to avoid convergence to a narrow area.

In Eq. (1), the crowding distance  $d_i$  is cumulative throughout generations. The crowding distance is calculated for each solution in the population during each iteration. Initially,  $d_i$  is set to zero, and then the summation term is added to account for the crowding distances across multiple objectives. This cumulative formulation ensures that the boundary solutions are preserved and the distribution of solutions along the Pareto front is enhanced. Specifically, for each individual  $i$  within a Pareto front, the summation term  $\sum_{m=1}^M \left( \frac{f_{m,i+1} - f_{m,i-1}}{f_m^{\max} - f_m^{\min}} \right)$  quantifies the

diversity of the solution by calculating the normalized difference between neighbouring objective values for all objectives  $M$ . The inclusion of  $d_i$  in the formula ensures that the crowding distance accumulates across multiple objectives, contributing to the selection of solutions that are well-distributed within the front. Thus,  $d_i$  is designed to be cumulative and is recalculated at every generation, ensuring dynamic adjustments to the solution set based on evolving objective values across generations.

## 2.4. Crowded comparison operator ( $\prec_n$ )

The crowded comparison operator selects solutions based on their dominance rank and crowding distance. The crowded comparison operator  $\prec_n$  is defined as Eq. (2):

$$i \prec_n j \text{ if } (NDR_i < NDR_j) \text{ or } (NDR_i = NDR_j \text{ and } d_i > d_j) \quad (2)$$

where:  $NDR_i$  and  $NDR_j$  represent the non-domination ranks of solutions  $i$  and  $j$ ,  $d_i$  and  $d_j$  are their respective crowding distances. The solution with a lower non-domination rank (better Pareto front) is favoured. If the ranks are equal, the one with a higher crowding distance (less crowded region) is selected. This operator helps balance convergence (by selecting solutions with lower domination ranks) and diversity (preferring solutions in less overcrowded areas). It ensures that MORIME generates well-distributed solutions across the Pareto front, preserving quality in both convergence and spread.

## 2.5. Best compromise solution (BCS)

The BCS is a method for selecting a balanced solution from the Pareto front that is useful for decision-makers facing conflicting objectives.

**Normalized Metric:** For each objective  $m$ , a normalized dominance score  $\mu_{i,j}$  for solution  $i$  is calculated as Eq. (3).

$$\mu_{i,j} = \frac{f_m^{\max} - f_{m,i}}{f_m^{\max} - f_m^{\min}} \quad (3)$$

Where  $f_m^{\max}$  and  $f_m^{\min}$  are the maximum and minimum values of the objective across the front,  $f_{m,i}$  is the objective value of the solution  $i$  in objective  $m$ . The BCS is the solution with the highest aggregated dominance score, balancing between conflicting objectives for a well-rounded result. BCS provides a practical solution when users need a single choice from a Pareto front, balancing multiple objectives to meet real-world requirements in MO optimization.

## 2.6. RIME-Specific steps for position update

MORIME integrates mechanisms inspired by the natural rime ice formation process to refine solutions toward optimal regions iteratively.

**Soft-Rime Search Strategy:** Encourages broad exploration in early iterations and is mathematically defined as per Eq. (4).

$$X_{i,j}^{\text{new}} = X_j^{\text{best}} + r_1 \cdot \cos(\theta) \cdot \beta \cdot (h \cdot (UB_j - LB_j) + LB_j) \quad (4)$$

where:  $X_j^{\text{best}}$  is the best solution found so far,  $r_1$  is a random variable for directional randomness,  $\cos(\theta)$  and  $\beta$  are factors that vary with iteration, guiding search behaviour over time.

The term  $h$ , as used in Eq. (4) of the MORIME algorithm, represents a scaling factor that modulates the step size of the soft-rime search strategy during solution updates. Specifically,  $h$  controls the extent of exploration by scaling the range of the solution space  $(UB_j - LB_j)$ , where  $UB_j$  and  $LB_j$  are the upper and lower bounds of the  $j$ -th decision variable, respectively. This factor is introduced to balance the trade-off between global exploration and local exploitation during the early iterations of the algorithm. In the context of the MORIME algorithm,  $h$  is not a predefined constant but is adaptively adjusted based on the iteration count or optimization requirements to ensure effective search

dynamics.

**Hard-Rime Puncture Mechanism:** Focuses on exploitation, updating solutions by selection probability described in Eq. (5).

$$X_{ij}^{new} = X_j^{best} \text{ if } r_3 < Fnorm(X_i) \tag{5}$$

where  $Fnorm(X_i)$  is a normalized fitness value for each solution, helping agents converge toward high-quality solutions. The RIME inspired updates balance exploration and exploitation, enabling MORIME to escape local optima and refine solutions across multiple objectives. MORIME

achieves this balance of diversity and convergence through this mathematical framework, and is therefore well suited to complex multi-objective optimization problems, including structural design and other engineering problems with multiple conflicting objectives.

The MORIME flowchart outlines a structured approach to optimizing and managing resources across multiple objectives in Fig. 1. It begins with an initialization phase, defining goals and constraints, followed by processing steps for evaluating solutions. The flow involves iterative optimization steps that assess solutions against predefined criteria, adjust parameters for improving outcomes, and select optimal

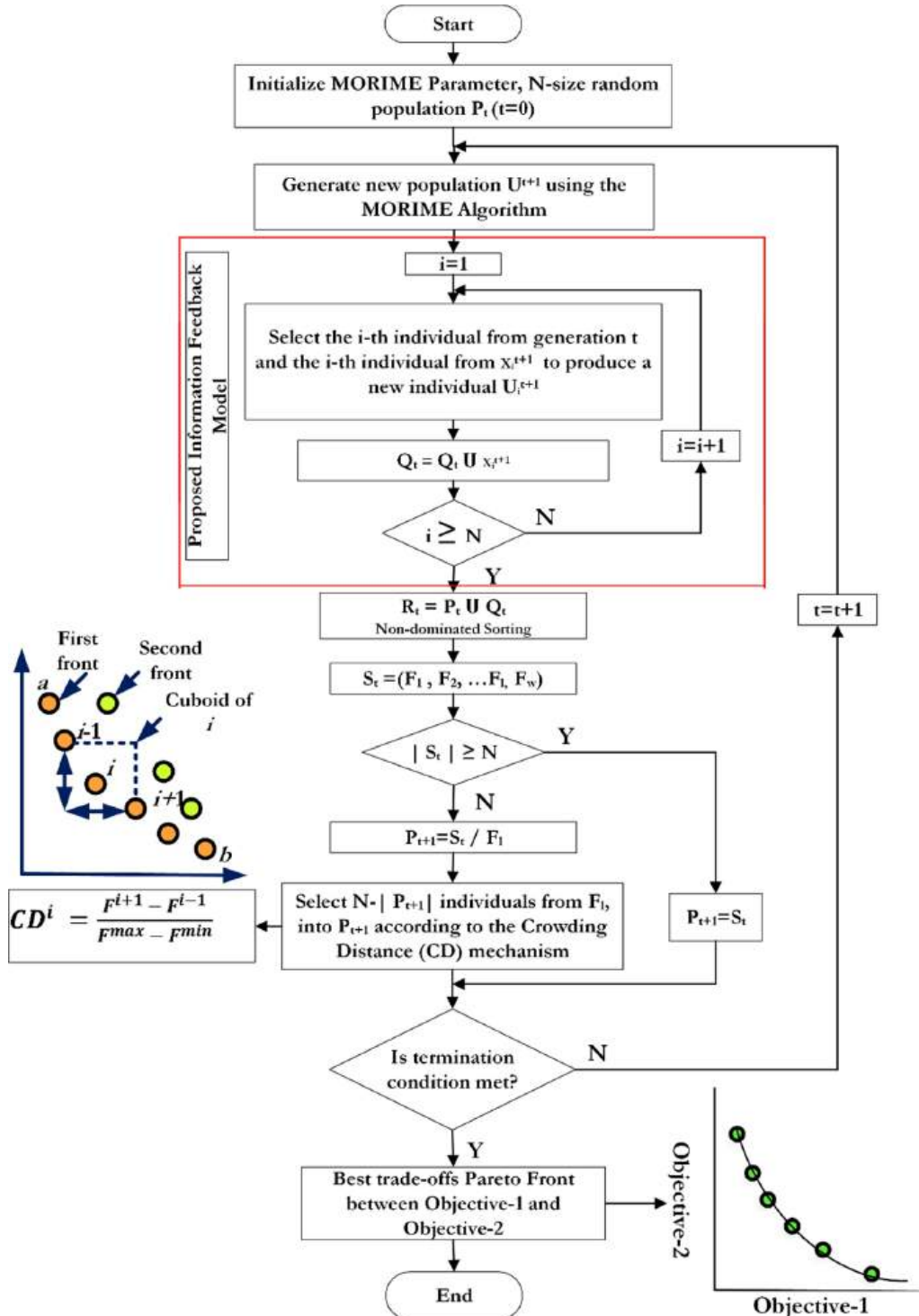


Fig. 1. Flowchart of MORIME.

configurations that satisfy MO requirements. The loop continues until a convergence criterion is met, resulting in a final set of robust, optimized solutions that effectively balance competing objectives.

### 3. Integrated FEA-Based truss optimization and multi-objective compliance assessment

This research investigates eight multi-objective truss sizing optimization problems: The trusses are 10-bar, 25-bar, 37-bar, 60-bar, 72-bar, 120-bar, 200-bar, and 942-bar [31]. The main objectives are to minimize structural weight and compliance while keeping designs below allowable stress limits. Eq. (6) is used to calculate structural weight, and Eq. (7) is used to calculate compliance, where displacement and loading vectors are calculated using finite element analysis (FEA).

$$Weight = \rho \sum_e A_e l_e \tag{6}$$

$$Compliance = U^T F \tag{7}$$

In these equations,  $\rho$  represents material density,  $A_e$  is the cross-sectional area of element  $e$ , and  $l_e$  is the length of element  $e$ . Each element stress must satisfy the allowable stress constraint as described in Eq. (8), where  $\sigma_{allowable}$  represents the maximum allowable stress for the material.

$$g = \max(\sigma_e - \sigma_{allowable}, 0) \tag{8}$$

Constraints in the truss bar optimization problem were handled using a penalty-based approach integrated into the objective function evaluation. For each candidate solution, a constraint violation measure  $C$  was calculated as the sum of all normalized violations of constraints (e.g., stress, displacement, and other limits). A penalized objective function was  $F_{penalized} = F_{objective} + \lambda \cdot C$ , where  $F_{objective}$  is the original objective value,  $C$  is the total constraint violation, and  $\lambda$  is a penalty coefficient that scales the impact of violations. Feasible solutions ( $C = 0$ ) were prioritized, while infeasible solutions ( $C > 0$ ) were penalized, ensuring adherence to all constraints. This method ensures that the algorithm emphasizes feasible regions of the solution space while optimizing the objectives effectively.

All test cases use consistent definitions for material properties: a density of  $7850 \text{ kg/m}^3$ , allowable stress of  $400 \text{ MPa}$ , and modulus of elasticity of  $200 \text{ GPa}$ . The design variables are discrete to reflect practical constraints in real-world truss sizing. Figs. 2-9 show the layout of each truss structure, including configurations for 10-bar, 25-bar 3-D truss, 37-bar, 60-bar, 72-bar 3-D truss, 120-bar, 200-bar, and the 942-bar tower truss. Some problems include grouped design variables, meaning the number of variables may not match the number of truss

members. The number of design variables for the 10-bar, 25-bar, 37-bar, 60-bar, 72-bar, 120-bar, 200-bar, and 942-bar problems are 10, 8, 15, 25, 16, 7, 29, and 59, respectively.

#### 3.1. Truss10bar

As per Fig. 2, this structure uses design variables for cross-sectional areas, denoted as  $A_i$  for  $i = 1, 2, \dots, 10$ . The stress constraint is set to  $\sigma_{allowable} = 400 \text{ MPa}$  with a material density  $\rho = 7850 \text{ kg/m}^3$  and Young modulus  $E = 200 \text{ GPa}$ . The size variable  $S$  can vary from  $[1, 1.5, 2, \dots, 21] \cdot 10^{-3} \text{ m}^2$ . The loading condition involves forces at nodes 2 and 4 with a  $1000 \text{ KN}$  downward direction.

#### 3.2. Truss25bar

This truss, demonstrated in Fig. 3, also adheres to a stress constraint of  $\sigma_{allowable} = 400 \text{ MPa}$  and uses the same density and Young modulus as the 10-bar truss. The design variables are similarly defined, but the loading condition is more complex, involving multiple forces at various nodes. This structure requires optimization to handle the increased loading points while minimizing weight and compliance.

#### 3.3. Truss37bar

Fig. 4 shows that the 37-bar truss has the same material properties and stress constraints as the previous trusses. It introduces multiple load cases[32] with  $1000 \text{ KN}$ . The design variables remain within the range  $[1, 1.5, 2, \dots, 21] \cdot 10^{-3} \text{ m}^2$ .

#### 3.4. Truss60bar

This structure follows the same material and stress constraints with design variables ranging in size from  $[1, 1.5, 2, \dots, 21] \cdot 10^{-3} \text{ m}^2$ . The loading conditions involve multiple cases [32]. With forces applied across different nodes, optimizing for weight and stress distribution is essential. Fig. 5 shows 60-bar ring truss structures.

#### 3.5. Truss 72bar tower 3-D truss

Similar to the 60-bar truss, the 72-bar truss shown in Fig. 6 operates under the same stress constraints ( $\sigma_{allowable} = 400 \text{ MPa}$ ), density ( $\rho = 7850 \text{ kg/m}^3$ ), and Young modulus ( $E = 200 \text{ GPa}$ ). The size variable  $S$  ranges from the same as in previous cases. The loading conditions involve two cases, with complex force applications across the structure, necessitating a high optimization level [32].

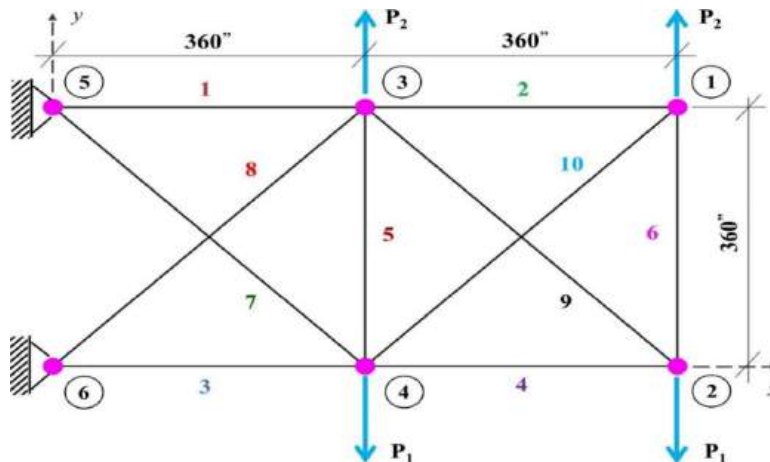


Fig. 2. Truss10bar.

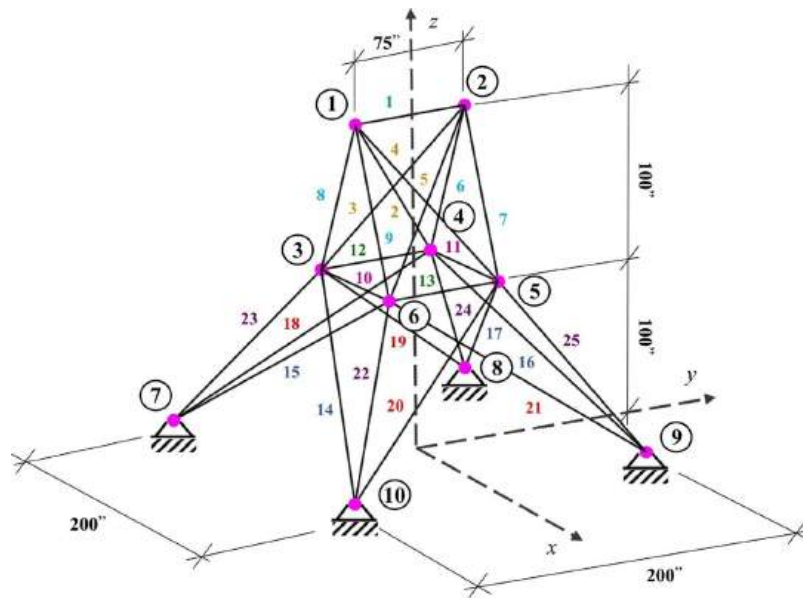


Fig. 3. Truss25bar.

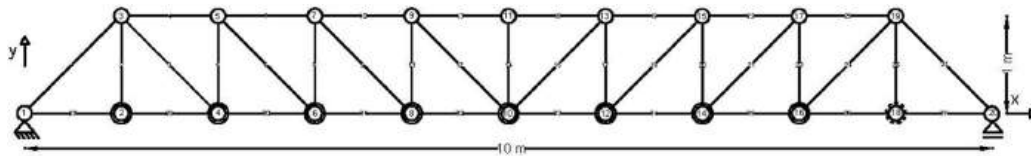


Fig. 4. Truss37bar.

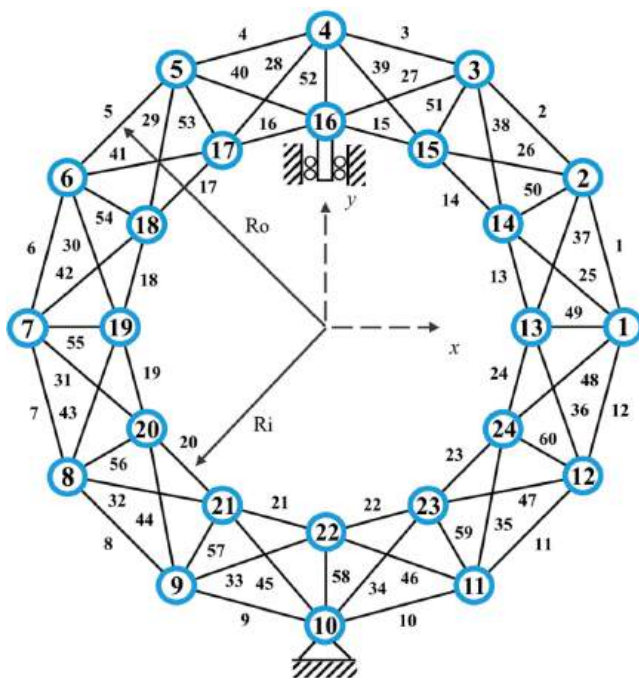


Fig. 5. Truss60bar ring.

### 3.6. Truss120bar dome truss

This truss continues with the same stress, density, and Young modulus constraints. However, the design variables  $S$  include a range of

$[1, 1.5, 2, \dots, 21] * 10^{-3} m^2$ . The structure faces various loading conditions involving different force magnitudes at nodes, which requires careful optimization to ensure structural performance under heavy loads [32]. The 120-bar dome truss ground structures are indicated in Fig. 7.

### 3.7. Truss200-bar

Like the other trusses, the 200-bar truss follows the same stress ( $\sigma_{allowable} = 400 \text{ MPa}$ ), density ( $\rho = 7850 \text{ kg/m}^3$ ), and Young modulus ( $E = 200 \text{ GPa}$ ) constraints. The size variable  $S$  ranges from the same as the previous cases. This structure is subject to lateral and vertical loadings at multiple nodes, increasing the complexity of the optimization process. Fig. 8 shows a 200-bar truss.

### 3.8. Truss942bar tower structure

Fig. 9 shows a highly complex tower truss structure under various loading conditions. Like the others, this truss operates under stringent material constraints, with maximum allowable stress, density, and Young modulus consistent across all truss structures in this optimization study. Cross-sectional areas represent the design variables for the 942-bar truss  $A_i$  for  $i = 1, 2, \dots, 942$ . The cross-sectional areas can vary within a predefined set of discrete values, the same as in previous cases, indicating larger potential sizes compared to smaller trusses. The more extensive range of cross-sectional areas accommodates the significant structural demands placed on this truss due to its size and complexity.

The 942-bar truss loading conditions are broken up into several sections with specific vertical and lateral force specifications. Section 1 applies vertical loadings at different nodes. Section 2 includes vertical loadings at various points and Section 3 is associated with lateral loading conditions on the right hand and left hand sides of the truss. The magnitudes of lateral loading are significant, making the design

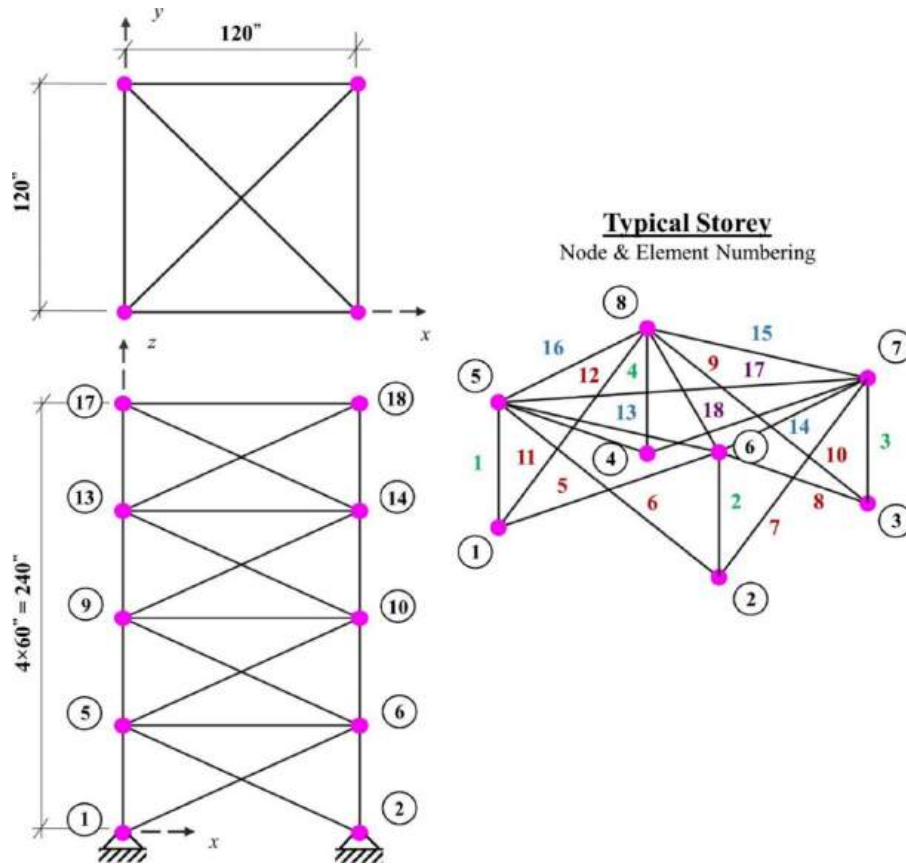


Fig. 6. The 72-bar 3D truss.

optimization more complex. For instance, the truss is subjected to lateral loadings of  $P_x = \pm 3$  KN and a vertical loading of  $P_z = -100$  KN to make sure that the truss can resist both vertical and horizontal loads at the same time.

#### 4. Computational analysis and performance evaluation

Rigorously comparing the MO algorithms requires evaluation of proper performance metrics. Four established metrics are employed: The Hypervolume (HV) indicator, Inverted Generational Distance (IGD), Spacing (SP), and computational efficiency are considered. The metrics offer a unique insight into algorithmic performance across convergence, spread, and overall solution quality.

##### 4.1. Hypervolume (HV)

The HV metric, given in Eq. (9), is the portion of the objective space covered by the non-dominated solution set [33]. The solutions cover a larger area of the objective space, and thus a higher HV value implies better performance. For each solution  $i$  in the set  $S$ , a hypercube  $V_i$  is defined in terms of a set of reference points. Each solution objective vector is separated from its closest reference point by the Euclidean distance  $d_i$ , which estimates the volume of objective space dominated by the Pareto front solutions. This measure allows us to evaluate the solution expansion and quality in the objective space.

$$HV = \text{volume} \left( \bigcup_{i=1}^A V_i \right) \quad (9)$$

##### 4.2. Inverted generational distance (IGD)

Quantitatively, the obtained Pareto front can be test with the IGD

represented by Eq. (10) to approximate how close the obtained Pareto front is to the original Pareto front. Calculates as the average of the Euclidean distance from each point on the generated Pareto to its closest neighbor point in the actual Pareto [34]. Convergence is better if the IGD values are lower, since in this way the solutions are proximal to the ideal Pareto front. The related metric that has been proposed is  $|P'|$ , the number of solutions on the reference plane, measuring the front expansion and how close the front is to the true Pareto optimal set.

$$IGD = \frac{\sqrt{\sum_{i=1}^{nt} (d_i^2)}}{|P|} \quad (10)$$

Where  $d_i$  is difference between solution point from the reference Pareto front  $P'$  and obtained Pareto front  $P$  and  $nt$  number of pareto optimal solutions.

##### 4.3. Spacing (SP)

The metric, SP metric (as shown in Equation 14) assesses the distribution and spread of solutions along the Pareto front. Variance in spacing between neighbouring solutions is calculated to assess uniformity across the front [35]. A lower SP value implies that the resulting Pareto front is more evenly distributed and extensive, both of which imply an efficient algorithm which can generate diverse and well spread non-dominated solutions. The SP metric uses the maximum ( $f_i^{\max}$ ) and minimum ( $f_i^{\min}$ ) values of the  $i^{\text{th}}$  objective function to normalize the objective values, providing a comparative basis for distribution across multiple objectives.

$$SP = \frac{1}{|P| - 1} \sum_{i=1}^{|P|} (d_i - \bar{d})^2 \quad (11)$$

Where  $d_i$ : The distance between a solution  $i$  and its nearest neighbor

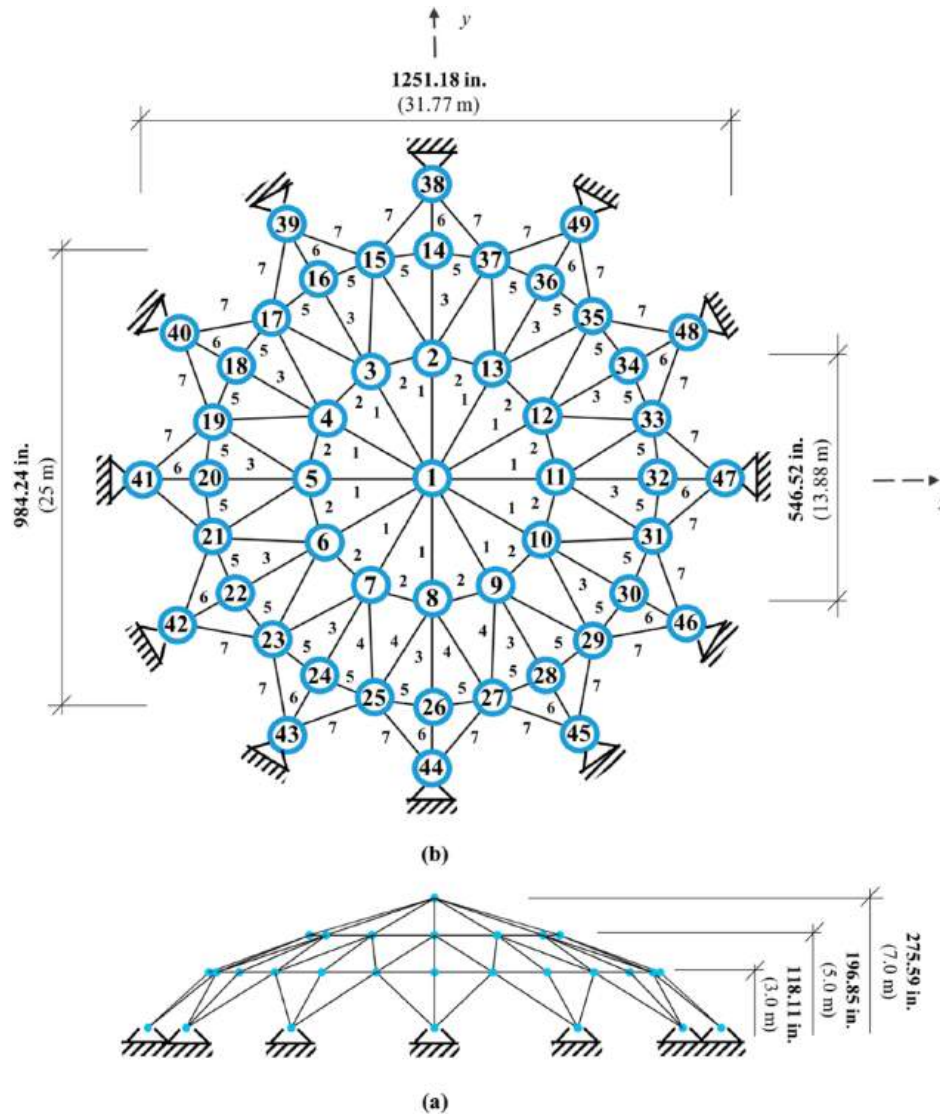


Fig. 7. The 120-bar truss.

in the obtained Pareto front,  $\bar{d}$ : The mean of all  $d_i$ , calculated as  $\bar{d} = \frac{1}{|P|} \sum_{i=1}^{|P|} d_i$  and  $|P|$ : The number of solutions in the obtained Pareto front. These metrics together provide a complete measure of the MO algorithm performance, allowing us to benchmark the MO algorithm with respect to other MO approaches in terms of solution quality, convergence and diversity of the Pareto front.

### 5. Comprehensive findings and comparative analysis

This study finds that MORIME is effective in solving complex structural optimization problems, especially in the truss design. Analysis shows that MORIME reliably generates well distributed Pareto optimal solutions with improved convergence for complex truss configurations. MORIME is benchmarked against leading multi objective optimization algorithms through comprehensive benchmarking and shows superior HV, IGD, and Spacing metrics performance. The metrics highlight MORIME ability to preserve solution diversity while quickly converging towards the Pareto front. Comparative evaluation demonstrates that MORIME is capable of balancing objectives, such as minimizing structural mass and compliance, and is more accurate and computationally efficient than traditional approaches. The robustness and adaptability of MORIME are demonstrated in this study, and MORIME is shown to be a

useful tool for multi-objective structural optimization.

In Figs. 10 to 17, the true Pareto fronts were obtained using a reference set of solutions generated by an exhaustive search or high-fidelity multi-objective optimization methods. In order to compute the reference Pareto fronts for smaller configurations, exhaustive sampling of the objective space under the defined constraints was used. For larger configuration, computationally intensive methods, like a combination of epsilon-dominance and clustering-based refinement, were used to approximate the true Pareto fronts. The convergence and diversity of these reference fronts were validated and they were suitable for benchmarking the obtained solutions.

#### 5.1. Optimal Pareto front analysis for truss structure MO optimization

Fig. 10 presents the Pareto fronts of different MO optimization algorithms NSGA-II, MOEA/D, MOMVO, MOTEO, MOLCA and the proposed MORIME algorithm for the 10-bar truss optimization problem. Objective functions  $f_1$  and  $f_2$ , key structural metrics such as mass and compliance, are plotted to illustrate the trade-offs achieved by each algorithm. MORIME shows a large convergence and a uniformly distributed Pareto front very close to the theoretical Pareto-optimal curve compared to other algorithms. Results from MORIME demonstrate that MORIME can balance the objectives while maintaining high diversity

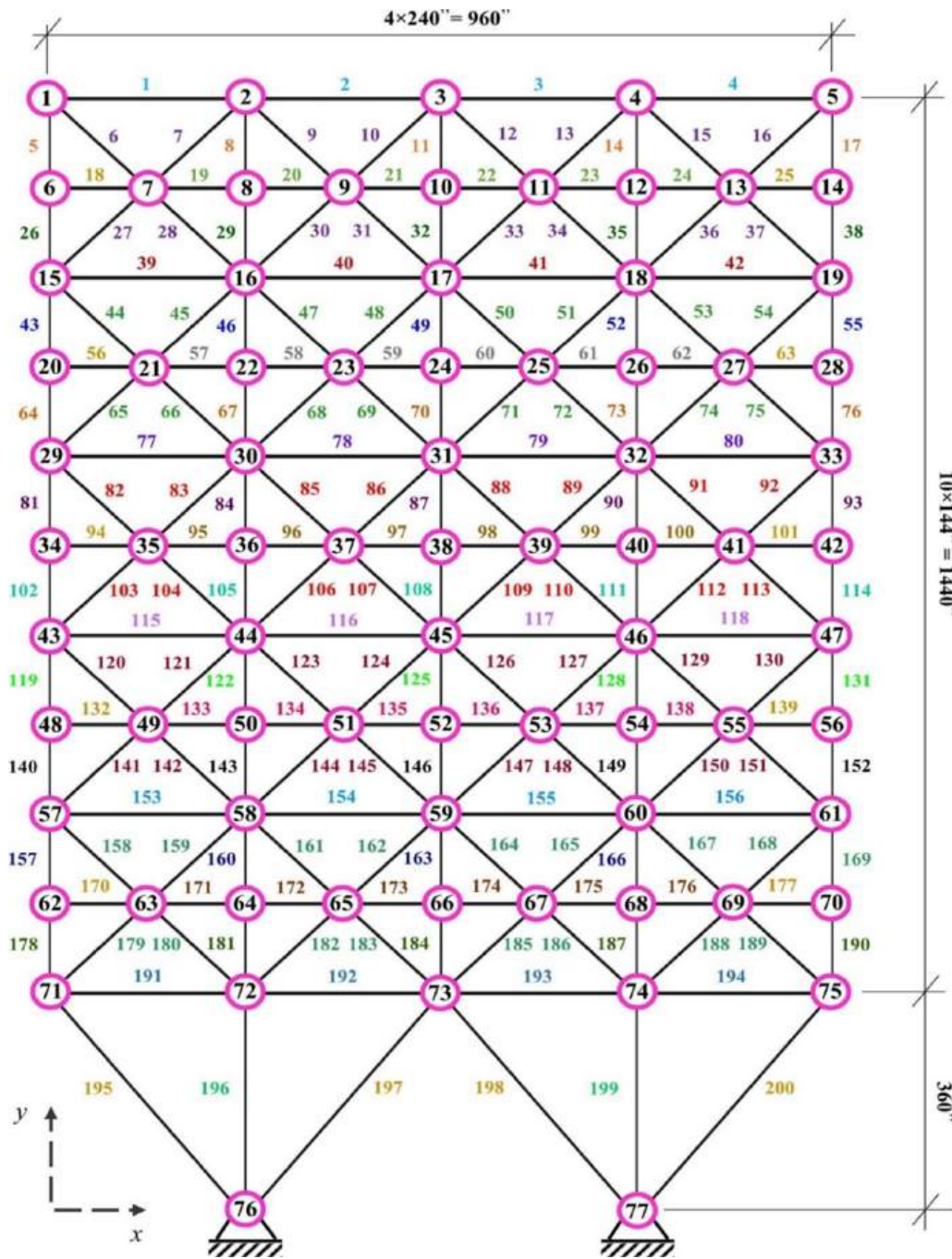


Fig. 8. The 200-bar truss.

among solutions and outperform traditional approaches like NSGAI and MOEAD. The comparison demonstrates that MORIME is more efficient in structural optimization, since it produces solutions that are very close to the optimal tradeoff curve, representing both better solution quality and robust diversity along the front.

Fig. 11 shows Pareto fronts of various MO optimization algorithms, applied to the 25-bar truss optimization problem, with weight and compliance being critical structural performance objectives. Our results from MORIME show excellent agreement with the theoretical Pareto optimal curve and demonstrate that MORIME is capable of converging to optimal solutions and providing a well distributed spread along the front. MORIME achieves a more balanced trade off between objectives than other algorithms, yielding a Pareto front that is both uniformly distributed and densely populated. This work demonstrates the

robustness and adaptability of our proposed approach, MORIME, to handle large complex structural optimization problems, returning solutions of high quality while maintaining diversity.

Fig. 12 shows the Pareto fronts for the 37-bar truss optimization problem for NSGA-II, MOEA/D, MOMVO, MOTEO, MOLCA, and the MORIME algorithm. MORIME shows a significant performance advantage in this challenging structural problem where objectives are to minimize weight and compliance. MORIME generates Pareto front that closely matches the ideal Pareto-optimal curve, and converges and distributes solutions better than other algorithms. The solutions spread achieved by MORIME shows its ability to achieve a good tradeoff between exploration and exploitation, maintaining diversity while approaching optimal tradeoffs. The evaluation of MORIME shows that it is capable of generating high quality, diverse solutions for complex MO

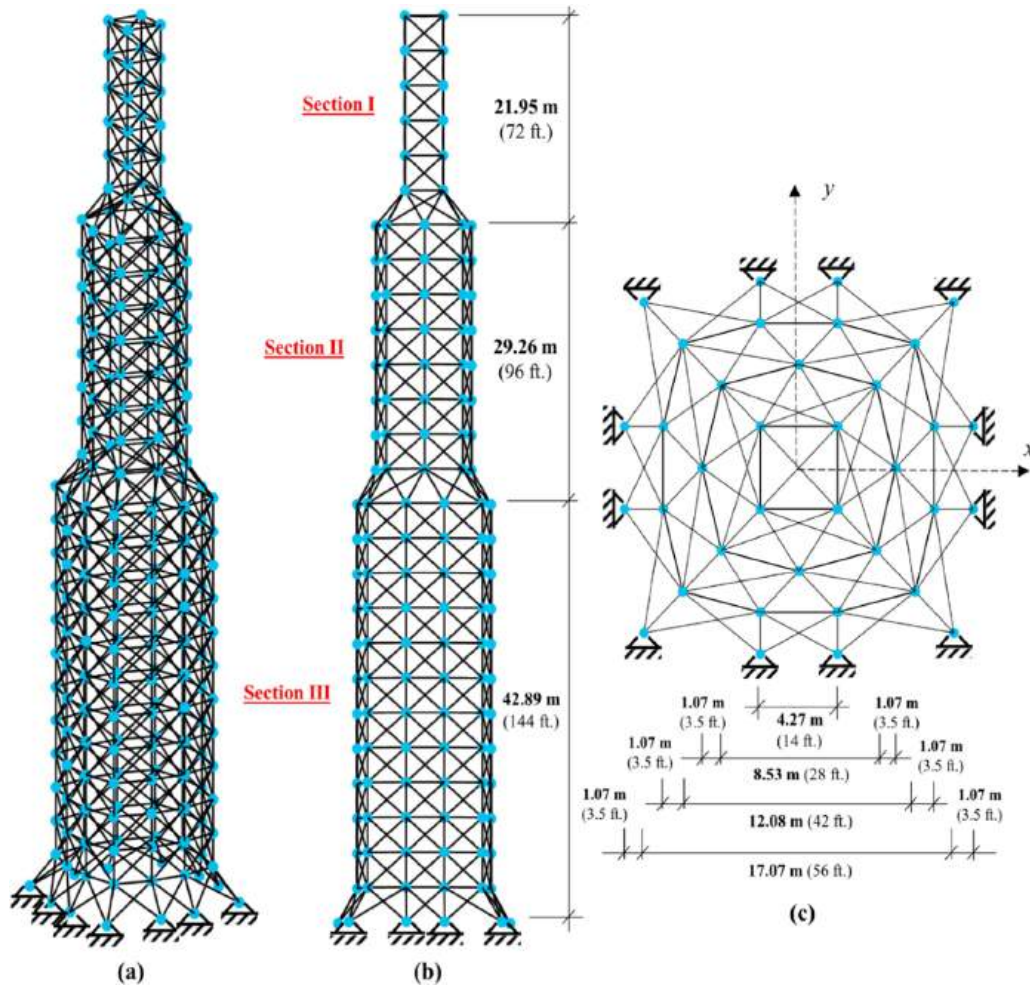


Fig. 9. Truss942bar tower.

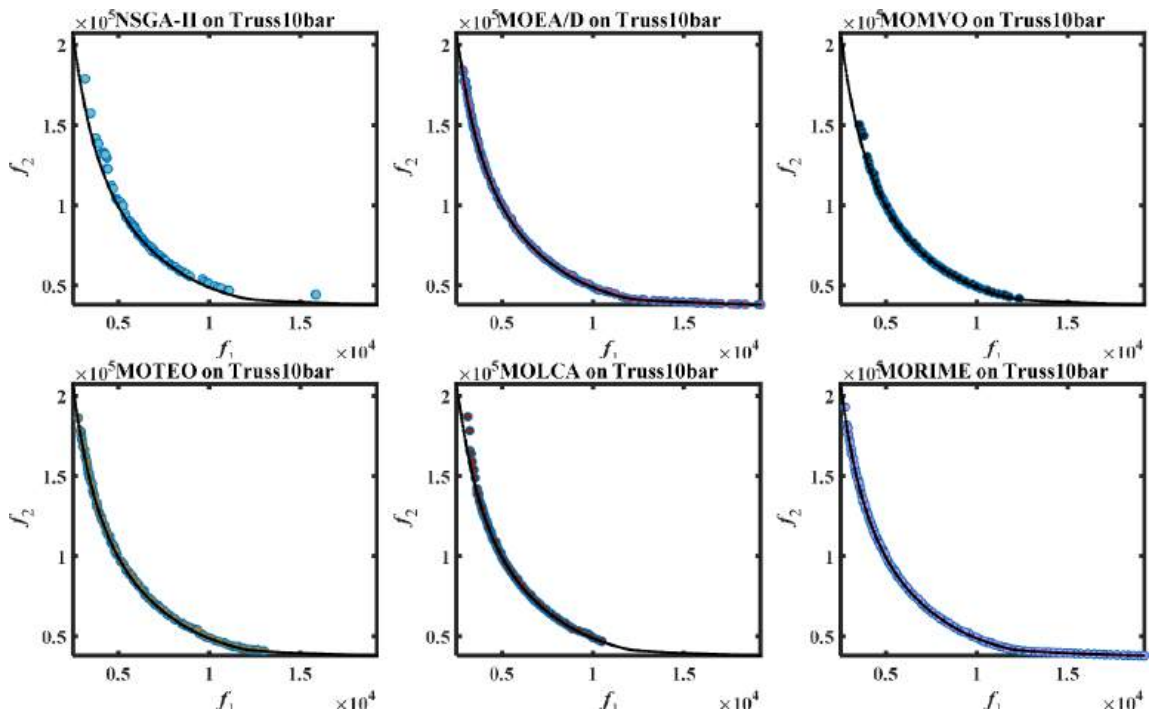


Fig. 10. Best Pareto fronts of 10-bar truss structures.

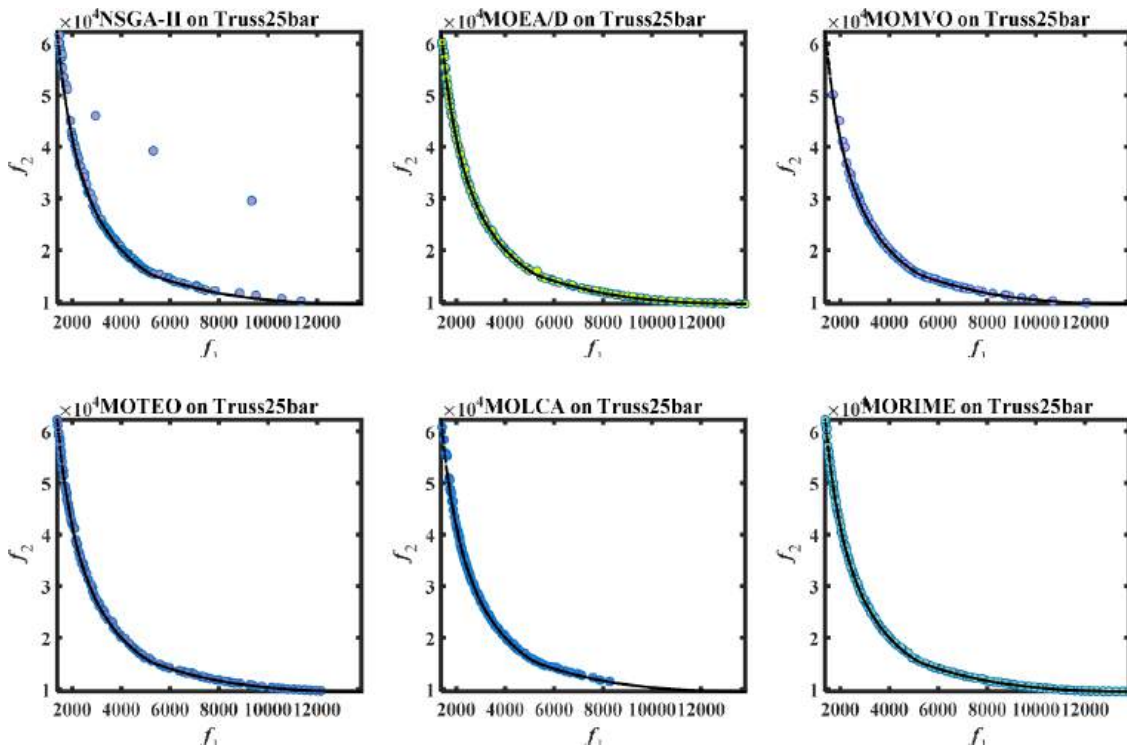


Fig. 11. Best Pareto fronts of 25-bar truss structures.

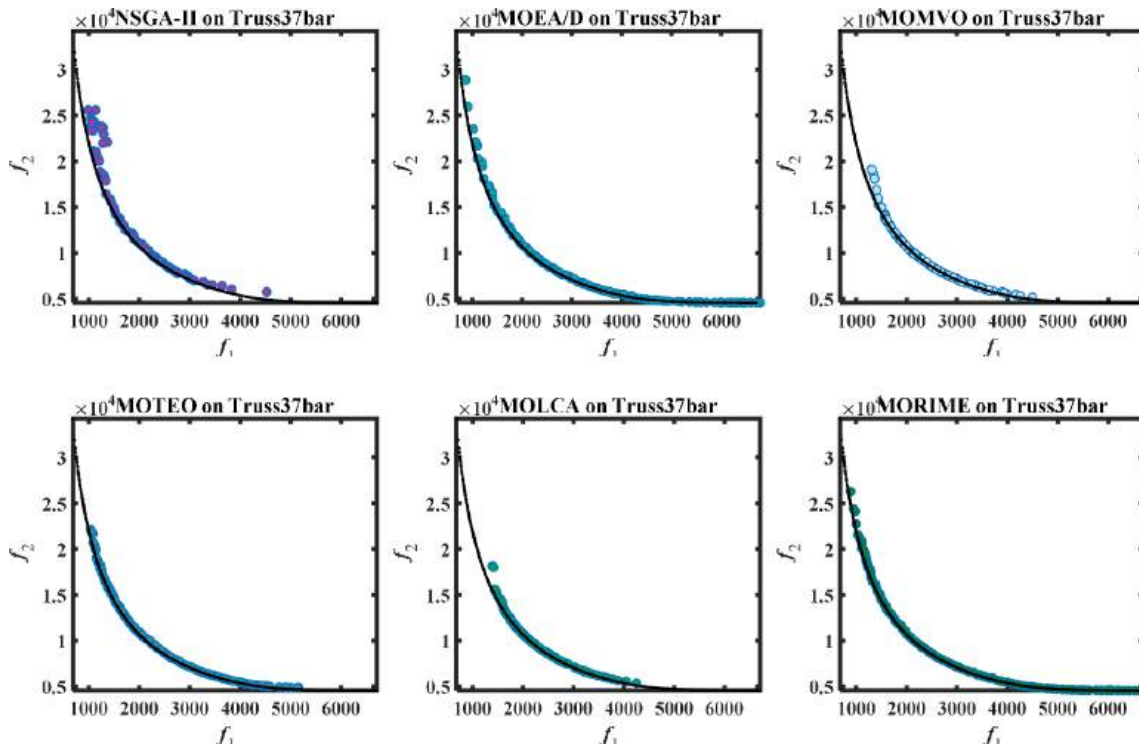


Fig. 12. Best Pareto fronts of 37-bar truss structures.

structural optimization problems.

The Pareto fronts for the 60-bar truss optimization problem are shown in Fig. 13, which also demonstrates the relative effectiveness of the algorithms under consideration. In this difficult MO scenario, where the objectives  $f_1$  and  $f_2$  aim at minimizing mass and structural compliance, MORIME clearly appears to be advantageous. MORIME achieves a

Pareto front that closely tracks the ideal curve, indicating good convergence as well as a well spread of solutions. The balance between diversity and convergence is what makes MORIME capable of exploring the solution space in depth, while making progress to the optimal trade-offs. Other algorithms, however, exhibit less consistent solution distributions, suggesting that they are not well suited to dealing with the

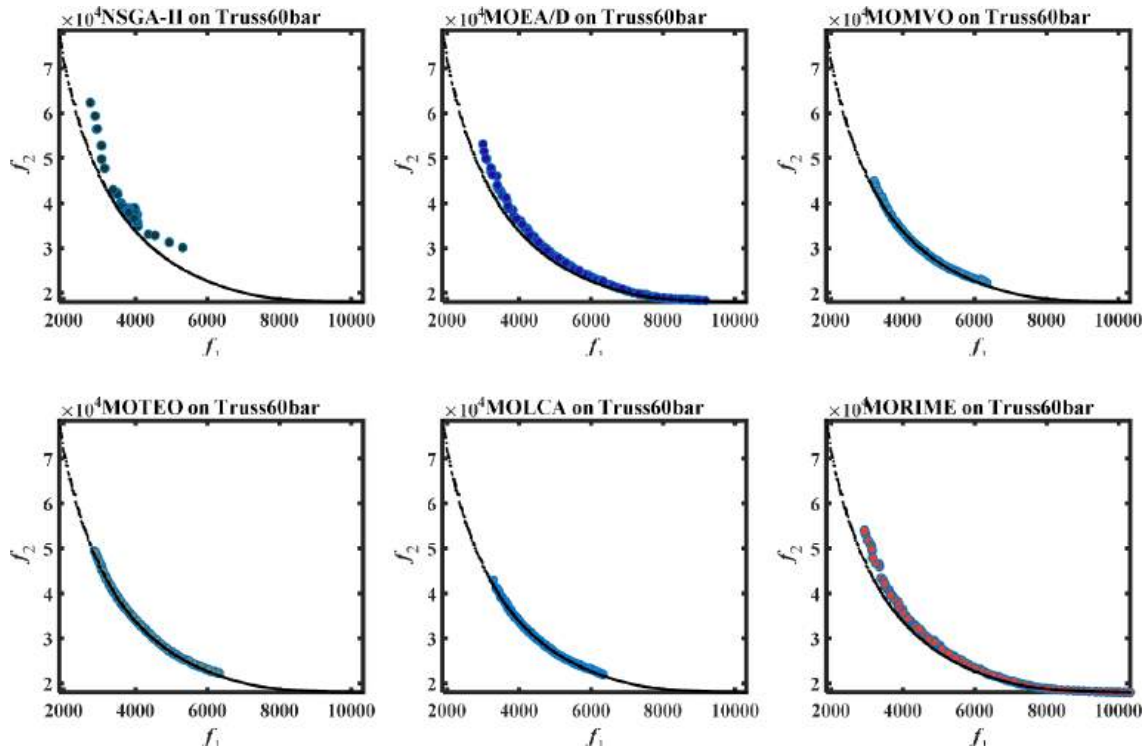


Fig. 13. Best Pareto fronts of 60-bar truss structures.

complexities of the 60-bar truss problem. These findings demonstrate the robustness and accuracy of MORIME making it well suited for complex MO structural optimizations, such as those necessary for 60 bar truss structures.

MORIME performance is strong in the 72-bar truss optimization problem shown in Fig. 14. Nevertheless, MOTEQ produces a significantly better result than other algorithms including NSGA-II, MOEA/D,

MOMVO, and MOLCA. In this case, the primary objectives are to minimize weight and compliance, typically conflicting objectives, and an effective algorithm must strike a balance between these. MORIME does a good job of aligning its Pareto front with the theoretical optimal front. The alignment of MORIME with the solution space demonstrates its capability to search the solution space quickly and find high quality tradeoffs that lead to an optimal balance between weight reduction and

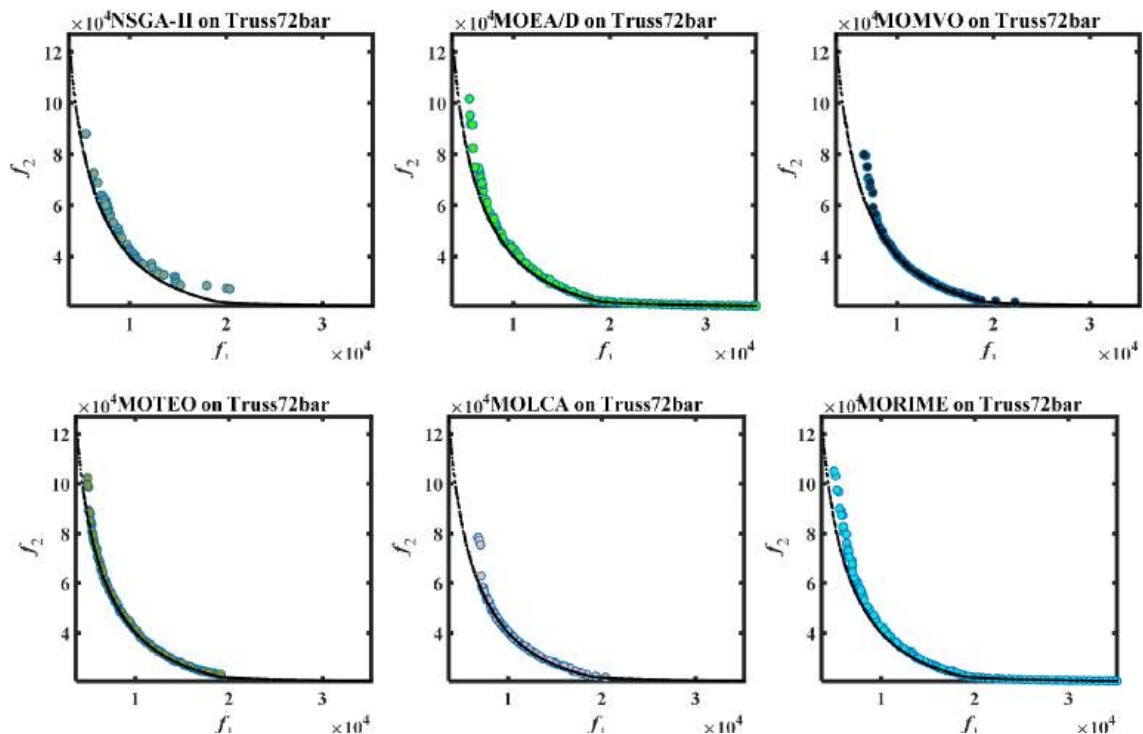


Fig. 14. Best Pareto fronts of 72-bar truss structures.

structural performance, a critical requirement in engineering applications. In addition to convergence, MORIME ensures a uniform distribution along the Pareto front, which is an important aspect of MO optimization that allows designers to obtain diverse, feasible solutions, improving flexibility to satisfy particular design needs. MORIME ability to strike a balance between diversity and convergence makes it a useful tool in such complex structural optimization tasks as the 72-bar truss, where a large number of intricate tradeoffs must be made. In addition to MORIME, this robust solution handles the MO challenges commonly found in structural and engineering applications where conflicting objectives require detailed and comprehensive optimization.

On the 120-bar dome truss structure (see Fig. 15), MORIME is shown to be highly effective at optimizing this complex structural problem, with strong convergence and a well distributed Pareto front. The 120 bar truss is a difficult optimization problem due to intricate load bearing requirements and geometric constraints, and an algorithm is needed to achieve high convergence and diversity. In addition, MORIME can maintain a uniform distribution along the Pareto front in the 120-bar dome truss optimization. MORIME has the advantage of providing a well spread set of solutions over the objective space, unlike NSGA-II and MOEA/D algorithms, which can show clustering and uneven solution distribution. The distribution provides engineers with a great deal of design flexibility, such that the tradeoff between structural efficiency and material cost, both critical in large structures such as dome trusses, can be made. MORIME is a robust tool for structural optimization due to its strength in balancing convergence and diversity in this high dimensional problem, and is a valuable insight and flexibility in applications where weight reduction and maximizing performance are critical design factors.

MORIME shows strong performance in optimizing the 200-bar truss structure, achieving a good balance between convergence and solution diversity that is essential in dealing with the complexity and high dimensionality of this problem. The two inherently conflicting objectives are to minimize truss weight and reduce compliance. MORIME is shown to converge to a Pareto front which is close to the theoretical optimal, and to find good tradeoffs between weight reduction and structural performance compared to other considered algorithms. In

addition, as shown in Fig. 16, MORIME has a uniform distribution of solutions along the Pareto front. It offers an even spread that gives engineers a large range of design choices, unlike other methods, which can result in clustering or gaps. The uniformity of these materials allows engineers to meet specific design requirements in a flexible way, promoting material efficiency and structural integrity. The ability of MORIME to balance convergence and diversity renders it a useful tool for large scale structural optimization tasks, especially in advanced engineering applications where multiple, conflicting objectives must be optimized simultaneously.

MORIME is an efficient solver for the 942-bar giant tower truss structure in that it converges quickly to optimal solutions while retaining a variety of design options along the Pareto front. This scenario is a challenging MO optimization problem due to the many design variables and complex interactions of the structure, especially when trying to balance weight minimization with compliance reduction. MORIME closely approximates the theoretical Pareto front, as shown in Fig. 17, with solutions deviating little from the ideal tradeoff curve. Unlike other algorithms that may generate sparsely populated or scattered fronts, MORIME provides a continuous and well distributed set of solutions, which provides decision makers with a wealth of viable design options. In engineering applications where robust design flexibility is crucial, this ability of MORIME to achieve a balanced distribution across the objective space significantly enhances its practical utility. In the high dimensional, complex setting of the 942 bar structure, MORIME demonstrates its effectiveness for large scale structural optimization, providing engineers with a useful tool for creating lightweight, stable designs that satisfy specific performance requirements.

## 5.2. Convergence performance assessment with HV metric

In Fig. 18, hypervolume (HV) convergence curves of optimizing different truss structures using multiple multi objective optimization algorithms such as NSGA II, MOEA D, MOMVO, MOTEO, MOLCA and MORIME are presented. The curves demonstrate how each algorithm efficiently explores the solution space and reaches optimal diversity and convergence on the Pareto front. The HV metric is a fundamental

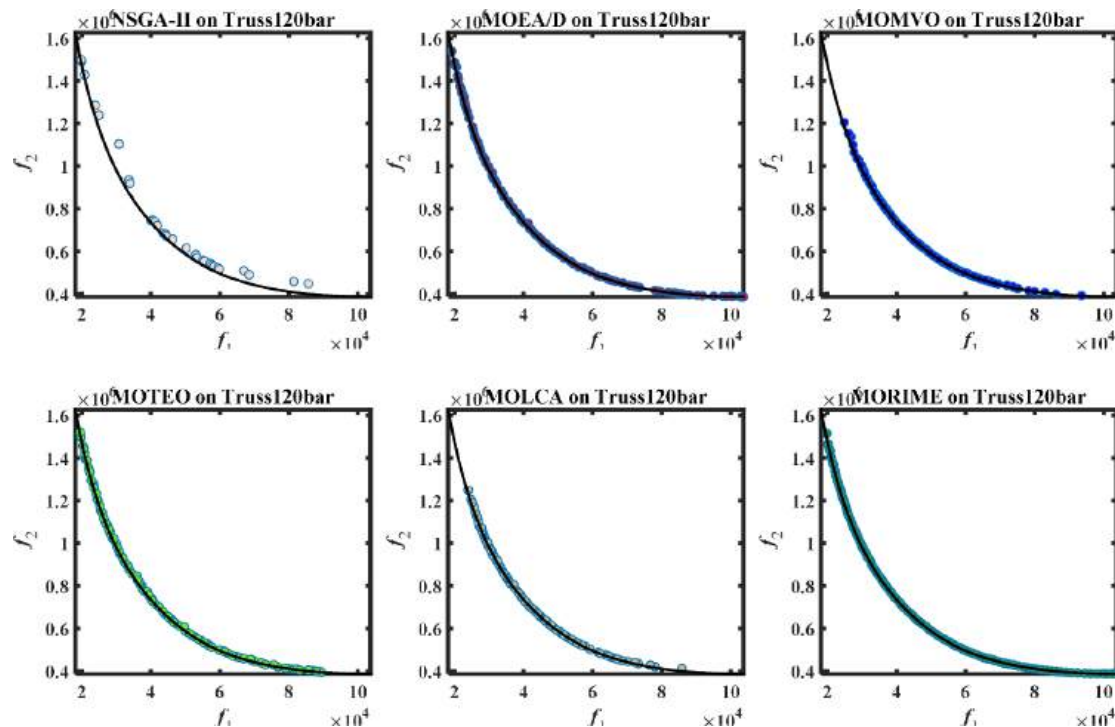


Fig. 15. Best Pareto fronts of 120-bar truss structures.

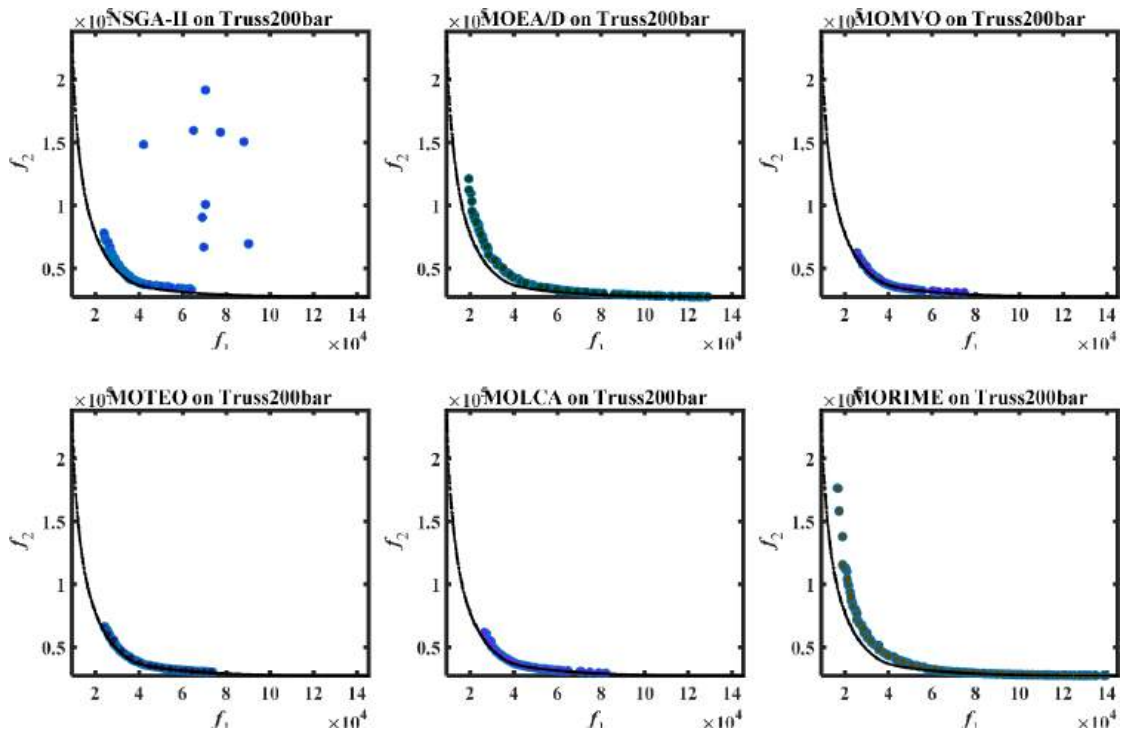


Fig. 16. Best Pareto fronts of 200-bar truss structures.

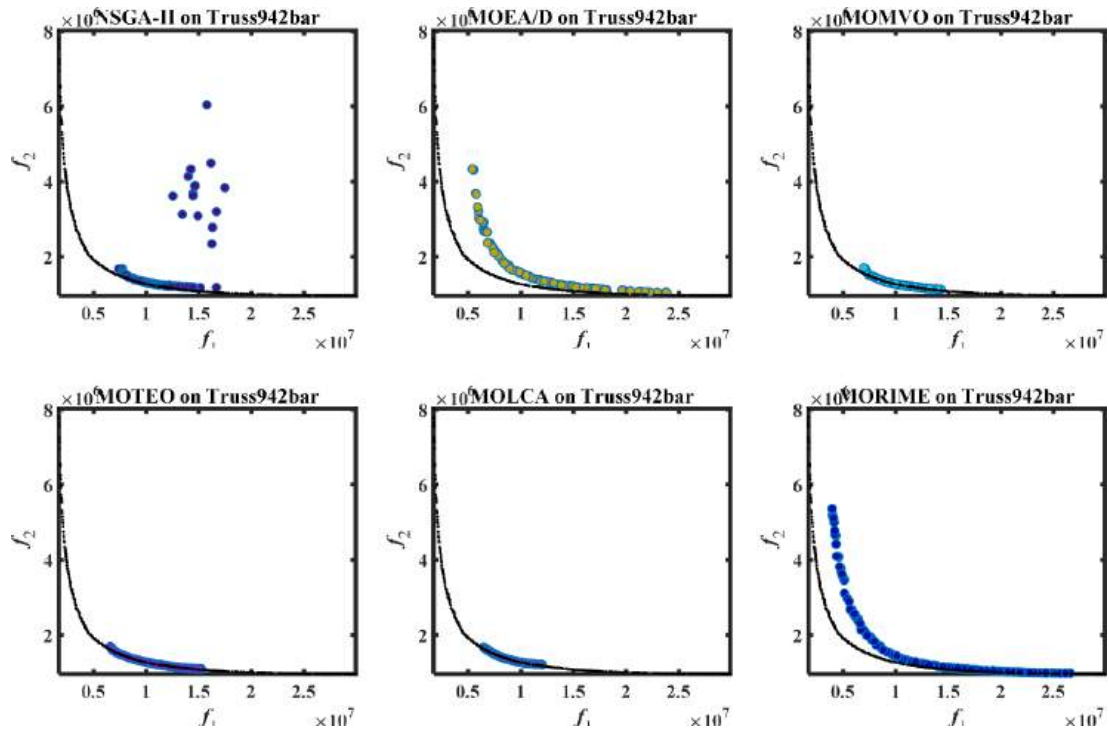


Fig. 17. Best Pareto fronts of 942-bar truss structures.

measure of the quality and diversification of the solutions with higher metric values corresponding to a better approximation of the Pareto front. In all truss configurations, MORIME shows good performance, frequently achieving high HV values more quickly than other algorithms. For example, MORIME converges rapidly in the 10 bar and 25 bar truss optimizations, achieving high HV values that indicate a balanced solution spread and strong convergence. The trend continues

in the more complex 37-bar and 60-bar truss optimizations, where MORIME is competitive in terms of HV with other high performing algorithms such as NSGA-II and MOEA/D. On the other hand, MOMVO and MOLCA are slower in convergence and HV levels.

The 120-bar dome truss structure (see Fig. 15) is shown to be highly optimized by MORIME, with strong convergence and a well distributed Pareto front on this complex structural problem. The 120 bar truss is a

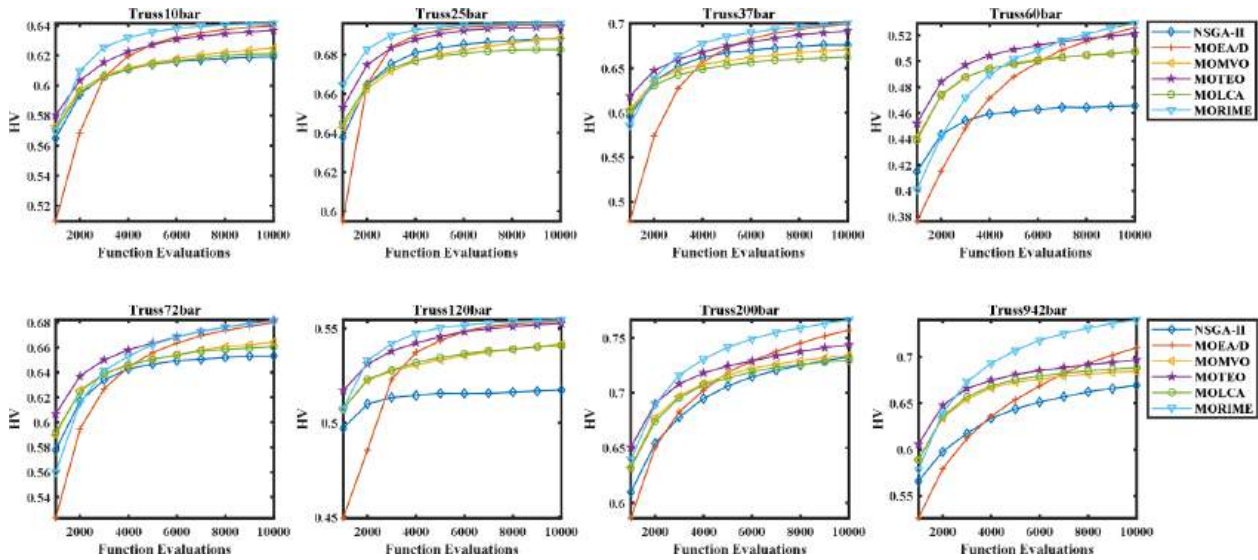


Fig. 18. Convergence curve of HV for all considered truss structures.

challenging optimization problem due to intricate load bearing requirements and geometric constraints, and an algorithm is needed to achieve high convergence and diversity. In addition, MORIME can maintain a uniform distribution along the Pareto front in the 120-bar dome truss optimization. MORIME offers a well spread set of solutions in the objective space compared to NSGA-II and MOEA/D algorithms which can display clustering and uneven solution distribution. The distribution provides engineers with a wide range of design options for the tradeoff between structural efficiency and material cost, two critical factors in large structures such as dome trusses. MORIME has the strength to balance convergence and diversity in this high dimensional problem and is a robust tool for structural optimization in applications where reducing weight and maximizing performance are critical design factors.

Table 1 summarizes the hypervolume (HV) results for eight truss structures optimized using six algorithms: The algorithms used here are NSGA-II, MOEA/D, MOMVO, MOTEO, MOLCA, and MORIME. Standard deviations of the HV metric are presented for each algorithm to give insight into how well each algorithm is able to approximate the Pareto front, with higher HV values indicating better performance at capturing the tradeoff between objectives like structural weight and compliance. For these truss configurations, MORIME shows robust convergence and stability, and consistently achieves high HV values. For the 10-bar truss problem, MORIME obtains an HV of  $6.4145e-1$ , which is 0.21% better than MOEA/D and the best algorithm for this configuration. For the 25 bar truss, MORIME also achieves an HV of  $6.9603e-1$ , outperforming MOEA/D by 0.1%, showing that MORIME converges strongly to the optimal trade-off. MORIME achieves  $7.0030e-1$  in the 37-bar truss, a significant improvement over other algorithms, with a 0.1% higher HV than the next best MOEA/D. In the 60-bar truss, MORIME achieves an HV of  $5.2921e-1$ , which is also around 0.6% better than MOEA/D,

demonstrating MORIME efficiency in this high complexity case.

MORIME achieves an HV of  $5.5453e-1$  in the more prominent 120-bar truss optimization, slightly better than 0.1% than the next best MOEA/D, demonstrating its capability in balancing objectives. MORIME achieves an HV of  $7.6630e-1$  for the 200-bar truss, which is about 1.25% higher than MOEA/D, and is robust for larger, more complex configurations. For the challenging 942-bar truss problem, MORIME attains a hypervolume of  $7.3990e-1$ , slightly better than MOEA/D by 4.2%, demonstrating its ability to retain high quality solutions in large design spaces. The results show that MORIME is able to produce well converged and diverse solutions across different truss configurations. The algorithm consistently outperforms other multi objective optimization algorithms and is a powerful tool for complex structural optimization applications.

Fig. 19 displays boxplots of the hypervolume (HV) values for all considered truss structures, comparing the performance of different multi-objective optimization algorithms: NSGA-II, MOEA/D, MOMVO, MOTEO, MOLCA and MORIME. The HV metric is the quality and diversity of the solutions along the Pareto front and the higher the HV, the better the front approximation to the optimal one. These boxplots clearly show the performance variability of each algorithm on different truss problems. We show that MORIME is robust and reliably converges, as evidenced by the high HV values and low variation of MORIME across different configurations. In particular, MORIME has compact distributions with fewer outliers, which suggests stable performance and interesting solution space exploration.

For simpler truss structures, e.g., 10-bar and 25-bar configurations, MORIME achieves some of the highest HV values compared to other algorithms, e.g., NSGA-II and MOEA/D, which have larger spread and variance. In more complex cases, such as the 60 bar and 120 bar trusses, this trend persists as MORIME has higher HV values with lower variance.

Table 1  
The hypervolume (HV) of the considered truss structures.

Problem	M	D	NSGA-II	MOEA/D	MOMVO	MOTEO	MOLCA	MORIME
Truss10bar	2	10	$6.1920e-1 \pm 6.01e-3$	$6.4012e-1 \pm 2.46e-3$	$6.2489e-1 \pm 4.30e-3$	$6.3686e-1 \pm 2.30e-3$	$6.2125e-1 \pm 7.68e-3$	$6.4145e-1 \pm 9.64e-4$
Truss25bar	2	8	$6.8833e-1 \pm 2.06e-3$	$6.9535e-1 \pm 2.64e-4$	$6.8870e-1 \pm 3.51e-3$	$6.9436e-1 \pm 4.68e-4$	$6.8262e-1 \pm 6.81e-3$	$6.9603e-1 \pm 2.37e-4$
Truss37bar	2	15	$6.7630e-1 \pm 7.51e-3$	$6.9944e-1 \pm 6.72e-3$	$6.7080e-1 \pm 9.38e-3$	$6.9190e-1 \pm 5.42e-3$	$6.6248e-1 \pm 1.18e-2$	$7.0030e-1 \pm 4.44e-3$
Truss60bar	2	25	$4.6567e-1 \pm 1.62e-2$	$5.2589e-1 \pm 1.41e-2$	$5.0772e-1 \pm 9.44e-3$	$5.2143e-1 \pm 7.93e-3$	$5.0739e-1 \pm 8.70e-3$	$5.2921e-1 \pm 8.84e-3$
Truss72bar	2	16	$6.5335e-1 \pm 1.11e-2$	$6.7988e-1 \pm 7.19e-3$	$6.6445e-1 \pm 9.89e-3$	$6.8224e-1 \pm 5.24e-3$	$6.6064e-1 \pm 1.26e-2$	$6.8138e-1 \pm 5.40e-3$
Truss120bar	2	7	$5.1745e-1 \pm 1.42e-2$	$5.5394e-1 \pm 2.50e-3$	$5.4177e-1 \pm 4.73e-3$	$5.5259e-1 \pm 1.92e-3$	$5.4088e-1 \pm 5.73e-3$	$5.5453e-1 \pm 8.32e-4$
Truss200bar	2	29	$7.3286e-1 \pm 1.32e-2$	$7.5691e-1 \pm 1.21e-2$	$7.3408e-1 \pm 1.60e-2$	$7.4366e-1 \pm 1.51e-2$	$7.2927e-1 \pm 1.62e-2$	$7.6630e-1 \pm 1.14e-2$
Truss942bar	2	59	$6.6935e-1 \pm 1.72e-2$	$7.0970e-1 \pm 1.98e-2$	$6.8434e-1 \pm 1.24e-2$	$6.9668e-1 \pm 1.30e-2$	$6.8823e-1 \pm 1.22e-2$	$7.3990e-1 \pm 1.51e-2$

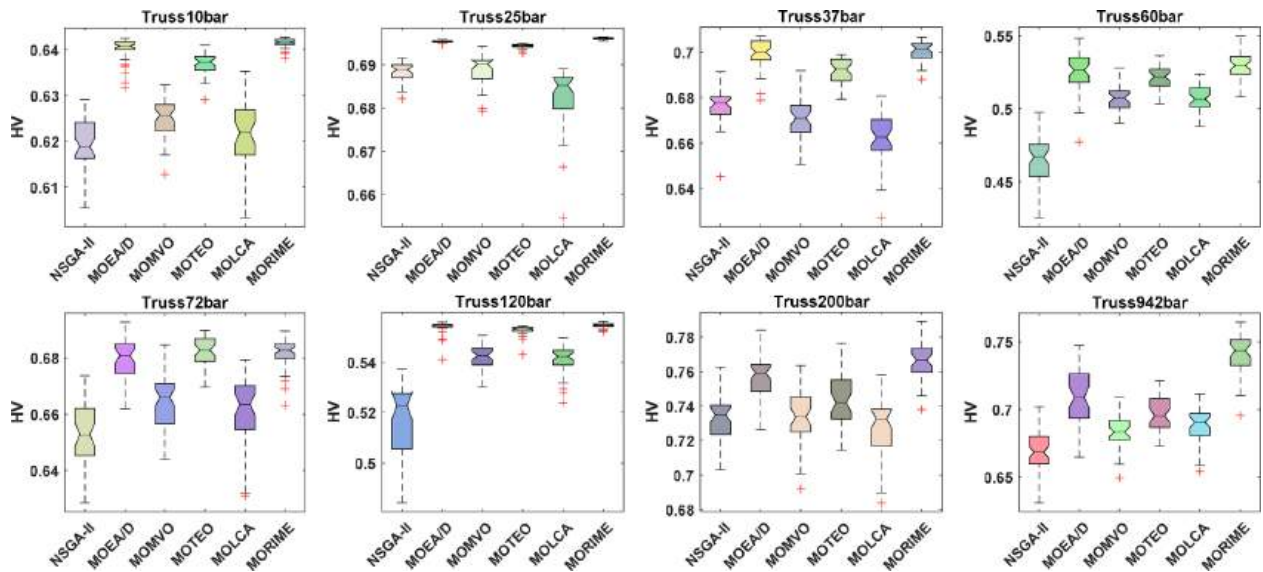


Fig. 19. Boxplots of HV for all considered truss structures.

However, other algorithms have larger spreads and more outliers with inconsistent performance. The MORIME distribution is highly clustered near the upper range of HV values for the highly complex 942 bar truss, demonstrating the capacity to handle convergence and diversity in high dimensional cases. The results confirm MORIME ability to produce high quality and stable solutions for different structural optimization problems. It is a reliable option for complex engineering applications where the solution diversity and consistency in performance are critical.

Table 2 presents the average HV ranks and corresponding *P*-values for eight truss optimization problems evaluated using six algorithms: MOEA/D, NSGA-II, MOMVO, MOTEQ, MOLCA, and MORIME. The lower the rank value, the better the algorithm performed in approximating the Pareto front, compared to the average rank values. These rankings are statistically significant (by their *P*-values): those with lower values mean that you can be more confident in the differences observed. In all configurations, MORIME has the highest average rank, indicating that it is the most capable method for optimizing complex truss structures. For example, in the 10-bar truss problem, MORIME achieves the highest average rank of 5.7317 (with significant *P*-value of 1.09E-36) among all algorithms. MORIME also shows its effectiveness in the 25-bar truss with an average rank of 5.9756, which is significantly better than other algorithms (*P* = 2.17E-38). For the 37-bar truss, MORIME also achieves an average rank of 5.4146, significantly better than the other algorithms (*P*-value of 1.57E-35).

In the more complex 60-bar truss problem, MORIME maintains a leading position with an average rank of 5.2439 and a *P*-value of 2.71E-30, reflecting its robust performance in high-dimensional optimization scenarios. For the 72-bar truss, MORIME rank of 4.9756 again highlights its efficiency in achieving high-quality solutions, supported by a *P*-value of 4.46E-29. In the intricate 120-bar truss case, MORIME attains a rank of 5.4634 (*P* = 6.19E-37). The 200-bar truss ranks 5.6341 with a *P*-value

of 4.26E-22, demonstrating its reliability in larger structural optimizations. Finally, in the complex 942-bar truss problem, MORIME secures the highest rank of 5.7317 with a *P*-value of 1.27E-25. These rankings and *P*-values confirm MORIME exceptional performance across various truss configurations. It consistently achieves optimal trade-offs and demonstrates a statistically significant advantage over other state-of-the-art algorithms in multi-objective optimization tasks.

### 5.3. Diversity analysis by IGD metric

Fig. 20 displays the convergence curves of the Inverted Generational Distance (IGD) metric for various truss structures, comparing the performance of NSGA-II, MOEA/D, MOMVO, MOTEQ, MOLCA, and MORIME. The IGD metric is a critical indicator of convergence quality, with lower values representing closer alignment to the true Pareto front and, thus, better optimization performance. Throughout the function evaluations, MORIME consistently achieves rapid convergence across different truss configurations, with IGD values steadily decreasing as the optimization progresses. In simpler truss problems, such as the 10-bar and 25-bar configurations, MORIME quickly reaches low IGD values, outperforming most other algorithms and indicating an efficient search and convergence process.

As the complexity increases in the 37-bar and 60-bar truss optimizations, MORIME demonstrates strong performance, achieving IGD values lower than or comparable to high-performing algorithms like NSGA-II and MOEA/D. In these cases, MORIME ability to maintain low IGD values highlights its effectiveness close to the actual Pareto front, reflecting its robustness in handling medium complexity. For more challenging structures, including the 120-bar and 200-bar trusses, MORIME maintains competitive IGD values, consistently converging faster than algorithms like MOTEQ and MOLCA. In the highly complex

Table 2  
The HV Average Ranks and *P*-values of the considered truss structures.

Problem	NSGA-II	MOEA/D	MOMVO	MOTEQ	MOLCA	MORIME	<i>P</i> VALUES
Truss10bar	1.6341	5.1951	2.5122	4.0488	1.878	5.7317	1.09E-36
Truss25bar	2.2439	5	2.3415	4.0244	1.4146	5.9756	2.17E-38
Truss37bar	2.6829	5.2683	2.0488	4.2439	1.3415	5.4146	1.57E-35
Truss60bar	1.0244	4.8293	2.7561	4.3415	2.8049	5.2439	2.71E-30
Truss72bar	1.561	4.6829	2.6585	5	2.122	4.9756	4.46E-29
Truss120bar	1.0976	5.2927	2.5122	4.1707	2.4634	5.4634	6.19E-37
Truss200bar	2.5366	4.6098	2.5854	3.4878	2.1463	5.6341	4.26E-22
Truss942bar	1.5854	4.4878	2.6098	3.6829	2.9024	5.7317	1.27E-25

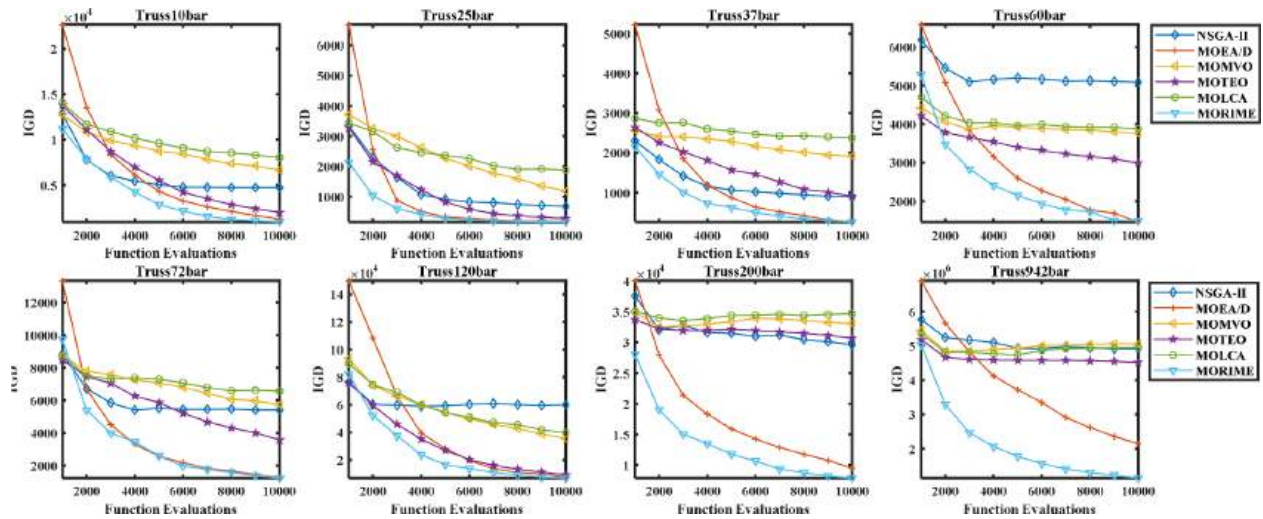


Fig. 20. Convergence curve of IGD for all considered truss structures.

942-bar truss, MORIME showcases its adaptability by achieving some of the lowest IGD values, underscoring its capability to manage convergence even in high-dimensional, complex optimization tasks. These IGD convergence curves affirm MORIME efficiency and reliability in achieving proximity to the optimal front across various truss structures, demonstrating its versatility as a robust algorithm for MO structural optimization.

Table 3 presents the IGD values for eight truss structures optimized using six algorithms: MOEA/D, NSGA-II, MOMVO, MOTEO, MOLCA and MORIME. IGD metric measures the convergence of the plotted Pareto fronts to an actual Pareto front where lower IGD means better convergence towards actual Pareto front and optimal solutions. The stability of each algorithm across multiple runs is reflected by a standard deviation of each IGD value.

For the 10-bar truss problem, MORIME has the lowest IGD of  $9.5582e+2$  and converges better than other algorithms with the least deviation from the true Pareto front. For the 25-bar truss, MORIME records an IGD of  $1.6867e+2$ , which is slightly better than MOEA/D, demonstrating its precise convergence and stability. When the 37-bar truss is more complex, MORIME also achieves an IGD of  $2.6500e+2$ , which is very close to that of MOEA/D, demonstrating its robustness in high dimensional optimization. In the case of 60-bar truss, MORIME also works well with an IGD of  $1.4914e+3$ , slightly higher than MOEA/D, but better than MOTEO and MOLCA. For the 72-bar truss optimization, MORIME achieves an IGD of  $1.2364e+3$ , very close to that of MOEA/D, indicating its robustness in dealing with complex optimization

problems.

In more challenging cases, MORIME shows a strong convergence performance with slightly lower values than MOEA/D, such as in the 120 bar truss where the IGD is  $6.8672e+3$ . MORIME shows its stability and efficiency in larger truss structures, recording an IGD of  $7.8735e+3$  for the 200-bar truss, outperforming MOEA/D and other algorithms significantly. Finally, MORIME has an IGD of  $1.1377e+6$  in the highly complex 942-bar truss problem, lower than the other algorithms, showing its effectiveness in large scale optimization problems. The strong convergence capabilities of MORIME are underlined over a wide range of truss configurations. The low IGD values that it consistently achieves indicate its accuracy and reliability in multi objective structural optimization tasks.

Fig. 21 presents boxplots of the IGD values for all considered truss structures, comparing the performance of six multi-objective optimization algorithms: MOEA/D, NSGA-II, MOMVO, MOTEO, MOLCA, and MORIME. The IGD metric is an important indicator of convergence quality, which lower values signify higher congruency toward the actual Pareto front. MORIME shows strong convergence and stability across different truss configurations, achieving low IGD values with low spread. In more straightforward truss problems, MORIME IGD distribution is tightly clustered near the lower end of the scale, outperforming other algorithms such as NSGA-II and MOEA/D whose IGD distributions are much more variable and have higher median IGD values.

For the more complex structures, the 60-bar and 120-bar trusses, MORIME continues to demonstrate low IGD values with a relatively

Table 3  
The IGD of the considered truss structures.

Problem	M	D	NSGA-II	MOEA/D	MOMVO	MOTEO	MOLCA	MORIME
Truss10bar	2	10	$4.7397e+3 \pm 2.85e+3$	$1.2691e+3 \pm 8.50e+2$	$6.6735e+3 \pm 2.13e+3$	$1.9984e+3 \pm 1.03e+3$	$8.0330e+3 \pm 3.76e+3$	$9.5582e+2 \pm 3.55e+2$
Truss25bar	2	8	$6.8247e+2 \pm 2.33e+2$	$1.8701e+2 \pm 8.35e+0$	$1.1828e+3 \pm 7.20e+2$	$2.9261e+2 \pm 9.61e+1$	$1.8859e+3 \pm 1.18e+3$	$1.6867e+2 \pm 2.38e+1$
Truss37bar	2	15	$9.0166e+2 \pm 2.56e+2$	$2.6153e+2 \pm 1.35e+2$	$1.9199e+3 \pm 5.89e+2$	$9.1262e+2 \pm 3.71e+2$	$2.3773e+3 \pm 7.09e+2$	$2.6500e+2 \pm 1.28e+2$
Truss60bar	2	25	$5.0871e+3 \pm 1.05e+3$	$1.4592e+3 \pm 6.80e+2$	$3.7603e+3 \pm 8.10e+2$	$2.9933e+3 \pm 6.47e+2$	$3.8748e+3 \pm 8.01e+2$	$1.4914e+3 \pm 5.42e+2$
Truss72bar	2	16	$5.4228e+3 \pm 1.27e+3$	$1.2504e+3 \pm 4.37e+2$	$5.7447e+3 \pm 1.94e+3$	$3.5822e+3 \pm 1.04e+3$	$6.5715e+3 \pm 2.52e+3$	$1.2364e+3 \pm 3.85e+2$
Truss120bar	2	7	$5.9984e+4 \pm 3.37e+4$	$7.3814e+3 \pm 5.96e+3$	$3.5453e+4 \pm 1.64e+4$	$9.2362e+3 \pm 6.69e+3$	$3.9530e+4 \pm 1.94e+4$	$6.8672e+3 \pm 2.07e+3$
Truss200bar	2	29	$2.9596e+4 \pm 7.08e+3$	$9.5035e+3 \pm 2.80e+3$	$3.3065e+4 \pm 6.06e+3$	$3.0688e+4 \pm 6.56e+3$	$3.4707e+4 \pm 5.73e+3$	$7.8735e+3 \pm 2.64e+3$
Truss942bar	2	59	$4.9160e+6 \pm 4.74e+5$	$2.1508e+6 \pm 6.84e+5$	$5.0569e+6 \pm 3.60e+5$	$4.5098e+6 \pm 4.41e+5$	$4.9537e+6 \pm 3.43e+5$	$1.1377e+6 \pm 4.74e+5$

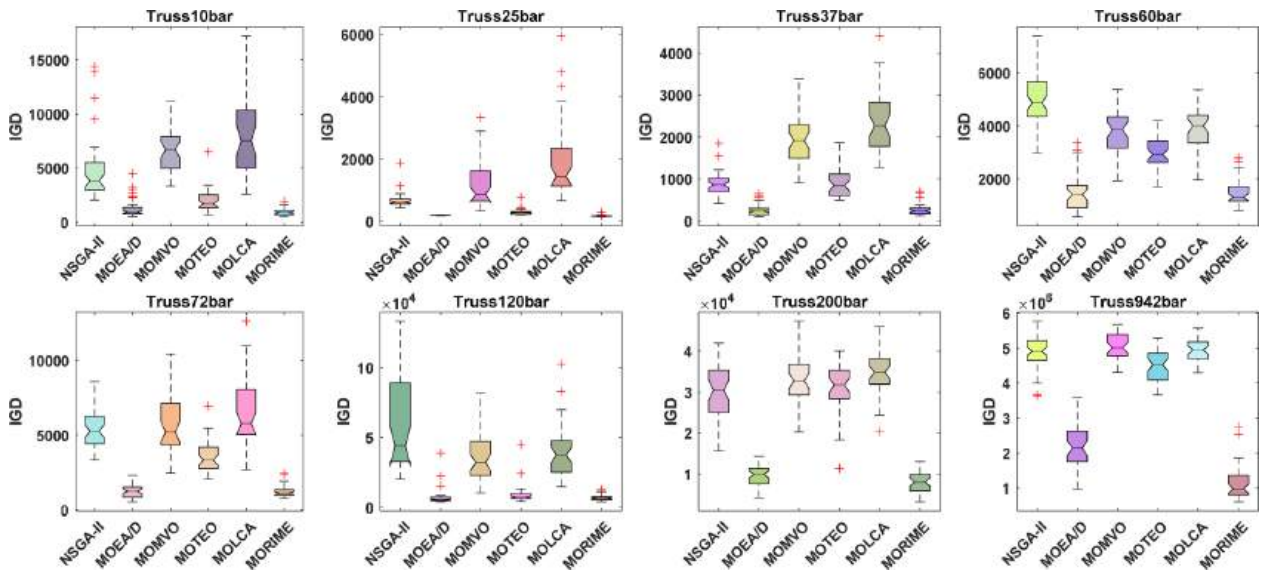


Fig. 21. Boxplots of IGD for all considered truss structures.

compact spread, indicating its robustness and adaptability to increasing problem complexity. In these cases, the spreads of other algorithms such as MOTEQ and MOLCA are larger and the outliers are higher, indicating less consistent convergence. MORIME boxplot for the highly complex 942-bar truss demonstrates low IGD values, showing that MORIME can efficiently approach the true Pareto front in high dimensional problems. The effectiveness of MORIME in delivering reliable and high quality solutions is evidenced by minimal outliers and narrow interquartile ranges across truss configurations. These boxplots overall confirm MORIME ability to get and stay close to the optimal front across different truss structures. It is a dependable choice for such complex structural optimization problems that stability and the convergence issue is sorely needed.

Table 4 displays the average ranks for the Inverted Generational Distance (IGD) values and corresponding *P*-values for eight truss structures optimized using six algorithms: MOEA/D, MOMVO, MOTEQ, MOLCA, and MORIME. MORIME has lower average ranks, which indicates better convergence performance, and is always ranked top in various configurations. In this case, *P*-values indicate the level of statistical significance of observed differences between the results obtained, and small values imply that confidence in superiority of results obtained should be strong.

In the 10-bar truss problem, MORIME achieves the best average rank of 1.5122 with a highly significant *P*-value of 5.20E-34, highlighting its strong convergence. Similarly, for the 25-bar truss, MORIME attains an impressive rank of 1.122, outperforming the other algorithms with a *P*-value of 2.38E-38. In the more complex 37-bar truss, MORIME maintains a competitive rank of 1.6098, supported by a significant *P*-value of 1.00E-36, emphasizing its consistency in multi-objective optimization. For the 60-bar truss, MORIME records a rank of 1.6341, closely aligned with MOEA/D and accompanied by a *P*-value of 2.50E-32, reflecting

MORIME strong performance in high-dimensional optimization. In the 72-bar truss case, MORIME achieves an average rank of 1.4146 with a *P*-value of 3.15E-32, indicating its stability and efficiency in maintaining a close approximation to the Pareto front.

In the more challenging 120-bar truss problem, MORIME secures a rank of 1.9268, demonstrating strong convergence with a significant *P*-value of 3.64E-32. For the 200-bar truss, MORIME continues to perform well, achieving a rank of 1.3415, further confirmed by a *P*-value of 4.20E-30, signifying its reliability for larger truss optimizations. Finally, in the highly complex 942-bar truss problem, MORIME achieves an average rank of 1.1463 with a *P*-value of 4.31E-32, indicating its capability to handle large-scale optimization tasks effectively. These results highlight MORIME robust convergence performance across various truss configurations. It consistently achieves top ranks and demonstrates a statistically significant advantage over other algorithms in complex multi-objective structural optimization tasks.

#### 5.4. Spacing and spread of solutions across the Pareto front

Fig. 22 displays the convergence curves of the Spacing (SP) metric for various truss structures, comparing the performance of six multi-objective optimization algorithms: MOEA/D, NSGA-II, MOMVO, MOTEQ, MOLCA, and MORIME. The issue of evaluating solution uniformity along the Pareto front is important and the SP metric is critical for the lower the SP the more evenly the solutions are spread from the Pareto front and also for better diversity among the solutions. MORIME is shown to converge well in spacing in each truss configuration, with progressively lower SP values as function evaluations increase. For simpler truss problems, such as the 10-bar and 25-bar trusses, MORIME quickly reaches low SP values, and the Pareto front is well distributed with small variation relative to other algorithms, which converge more

Table 4  
The IGD Average Ranks and *P*-values of the considered truss structures.

Problem	NSGA-II	MOEA/D	MOMVO	MOTEQ	MOLCA	MORIME	<i>P</i> VALUES
Truss10bar	4.2927	1.878	5.0976	2.7561	5.4634	1.5122	5.20E-34
Truss25bar	4.3171	1.9024	5	3.0244	5.6341	1.122	2.38E-38
Truss37bar	3.5122	1.4634	5.1951	3.561	5.6585	1.6098	1.00E-36
Truss60bar	5.6585	1.6098	4.4146	3.2439	4.439	1.6341	2.50E-32
Truss72bar	4.8537	1.5854	4.6341	3.4878	5.0244	1.4146	3.15E-32
Truss120bar	5.3659	1.6829	4.6098	2.5122	4.9024	1.9268	3.64E-32
Truss200bar	4.122	1.6585	4.6341	4.1951	5.0488	1.3415	4.20E-30
Truss942bar	4.5366	1.8537	5.1463	3.6585	4.6585	1.1463	4.31E-32

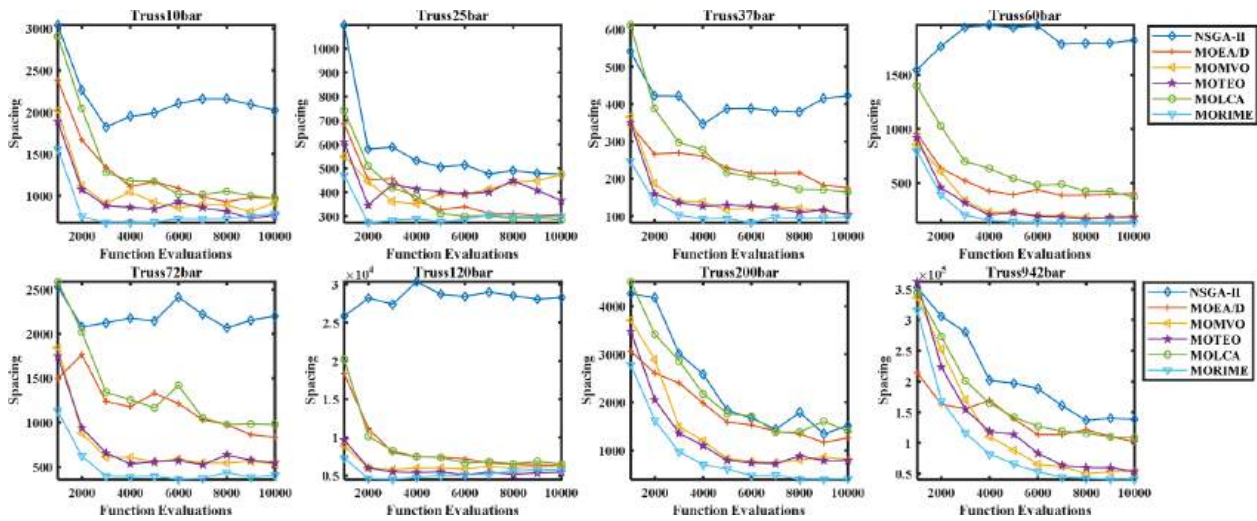


Fig. 22. Convergence curve of Spacing for all considered truss structures.

slowly or with larger fluctuations.

MORIME performs well in spacing for more complex trusses, e.g., the 37-bar and 60-bar structures, with lower SP values than high performing algorithms like NSGA-II and MOEA/D, which are less consistent in convergence. This trend demonstrates MORIME ability to provide a well distributed solution over a wide range of structural configurations. For the 120-bar and 942-bar trusses, as the truss structures become more complex, MORIME remains competitive, having some of the lowest SP values among all algorithms. It demonstrates its ability to preserve diversity and avoid solution clustering in high dimensional, complex problems. The MORIME SP convergence curves show that MORIME is capable of producing a balanced, evenly distributed Pareto front over a range of truss structures. In multi-objective engineering applications which require solution diversity and uniformity, it is a valuable tool for structural optimization tasks.

Table 5 presents the SP metric values for various truss problems optimized by six algorithms: MOEA/D, MOMVO, MOTEO, MOLCA, and MORIME. The lower value of the SP metric indicates a more uniform and well distributed spread of solution in the Pareto front. To account for the consistency of each algorithm performance, each SP value is reported along with its standard deviation. For the 10-bar truss problem, MORIME attains an SP of  $7.8074e+2$ , which is very close to MOTEO best value of  $7.6286e+2$ , indicating that MORIME is able to maintain a balanced spread across the Pareto front. MORIME records an SP of  $2.9836e+2$  for the 25-bar truss, which is slightly higher than MOLCA lowest value of  $2.8453e+2$ , but still good spacing performance.

As complexity increases in the 37-bar truss, MORIME achieves the lowest SP of  $9.7277e+1$ , outperforming all other algorithms and highlighting its superior solution distribution capabilities in a high-dimensional setting. In the 60-bar truss, MORIME performs well with an SP of  $1.3269e+2$ , demonstrating improved uniformity over other algorithms, such as MOTEO, which records an SP of  $1.8185e+2$ . For the 72-bar truss, MORIME attains an SP value of  $4.0199e+2$ , outperforming all algorithms except MOMVO and showcasing its ability to maintain diversity across the front. In the 120-bar truss problem, MORIME SP of  $5.7450e+3$  is the lowest among all algorithms, confirming its effective handling of more extensive, complex optimization scenarios.

For the 200-bar truss, MORIME has an SP of  $4.0874e+2$ , which is much lower than other algorithms, showing that it can maintain an even spread in complex truss structures. Lastly, MORIME yields an SP of  $4.0575e+4$  in the 942-bar truss, the lowest across all methods, demonstrating its robustness and adaptability for large scale optimization problems with diverse, high quality solutions. The SP results show that MORIME is capable of generating uniformly distributed solutions along the Pareto front, which makes it a useful tool for complex structural optimization problems where solution diversity is important.

Fig. 23 presents boxplots of the SP metric for all considered truss structures, comparing the performance of six multi-objective optimization algorithms: MOEA/D, NSGA-II, MOMVO, MOTEO, MOLCA and MORIME. The impact of the SP metric is on the uniformity of the solution distribution along the Pareto front such that lower SP values represent more evenly spread and higher diversity among solutions.

Table 5  
The Spacing (SP) metric values for the truss problems.

Problem	M	D	NSGA-II	MOEA/D	MOMVO	MOTEO	MOLCA	MORIME
Truss10bar	2	10	$2.0203e+3 \pm 1.03e+3$	$9.6861e+2 \pm 2.35e+2$	$9.1436e+2 \pm 2.80e+2$	$7.6286e+2 \pm 2.98e+2$	$9.6579e+2 \pm 1.96e+2$	$7.8074e+2 \pm 1.22e+2$
Truss25bar	2	8	$4.7521e+2 \pm 1.23e+2$	$3.0604e+2 \pm 3.18e+1$	$4.7215e+2 \pm 1.35e+2$	$3.6420e+2 \pm 1.32e+2$	$2.8453e+2 \pm 1.97e+1$	$2.9836e+2 \pm 2.61e+1$
Truss37bar	2	15	$4.2262e+2 \pm 3.23e+2$	$1.7570e+2 \pm 6.24e+1$	$1.0531e+2 \pm 2.91e+1$	$1.0386e+2 \pm 4.24e+1$	$1.6478e+2 \pm 6.58e+1$	$9.7277e+1 \pm 5.16e+1$
Truss60bar	2	25	$1.8218e+3 \pm 1.56e+3$	$4.0535e+2 \pm 2.04e+2$	$1.9421e+2 \pm 1.05e+2$	$1.8185e+2 \pm 1.26e+2$	$3.7122e+2 \pm 1.86e+2$	$1.3269e+2 \pm 4.02e+1$
Truss72bar	2	16	$2.2000e+3 \pm 1.49e+3$	$8.3660e+2 \pm 4.48e+2$	$5.3480e+2 \pm 1.92e+2$	$5.4492e+2 \pm 3.02e+2$	$9.7819e+2 \pm 5.07e+2$	$4.0199e+2 \pm 1.43e+2$
Truss120bar	2	7	$2.8273e+4 \pm 1.52e+4$	$6.3161e+3 \pm 1.04e+3$	$6.2647e+3 \pm 1.44e+3$	$5.4507e+3 \pm 1.60e+3$	$6.4706e+3 \pm 1.39e+3$	$5.7450e+3 \pm 6.37e+2$
Truss200bar	2	29	$1.5149e+3 \pm 9.06e+2$	$1.2636e+3 \pm 5.23e+2$	$8.0641e+2 \pm 4.44e+2$	$7.9172e+2 \pm 3.27e+2$	$1.4036e+3 \pm 8.46e+2$	$4.0874e+2 \pm 3.01e+2$
Truss942bar	2	59	$1.3843e+5 \pm 7.98e+4$	$1.0154e+5 \pm 2.41e+4$	$5.4453e+4 \pm 2.16e+4$	$5.3582e+4 \pm 1.98e+4$	$1.0809e+5 \pm 1.88e+4$	$4.0575e+4 \pm 1.35e+4$

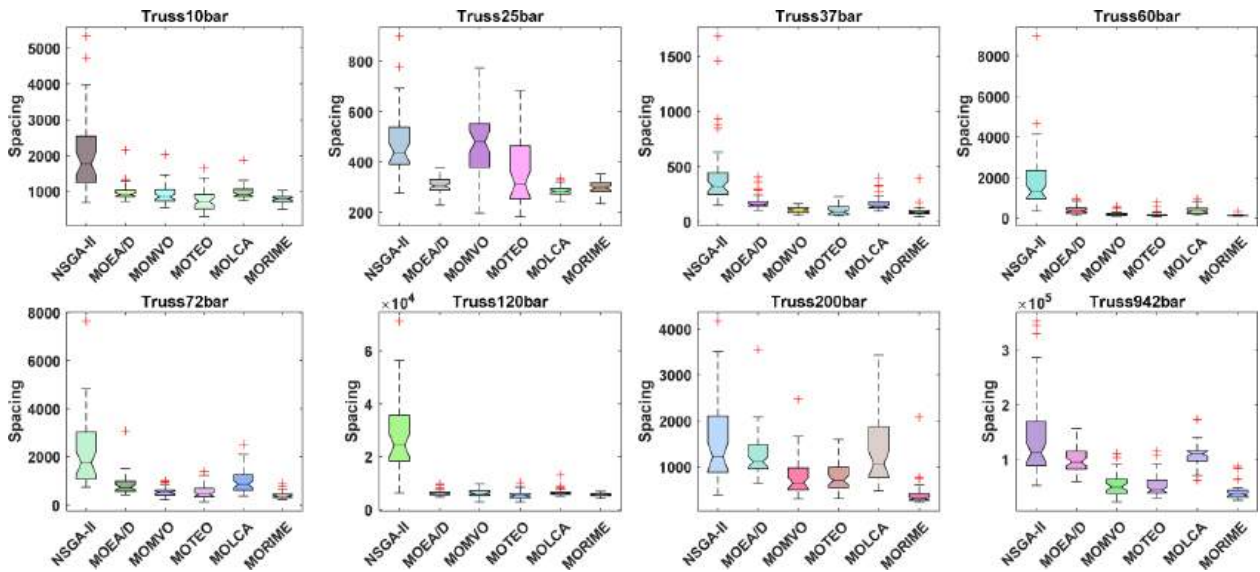


Fig. 23. Boxplots of Spacing for all considered truss structures.

MORIME shows low SP values with little variation across different truss configurations, demonstrating its ability to generate an evenly distributed Pareto front. For simpler truss structures, e.g., 10-bar and 25-bar trusses, MORIME exhibits a tightly clustered SP distribution at the lower end, outperforming most other algorithms. This result reflects the stability of MORIME in guaranteeing a well spread solution set early in the optimization process.

For the 37 and 60 bar trusses, MORIME has low SP values and a relatively narrow interquartile range, demonstrating robustness in handling diversity in higher dimensional problems. NSGA-II and MOEA/D exhibit more variability and outliers, suggesting poorer spacing performance over the front. MORIME performs well for the highly complex trusses, namely the 120-bar and 942-bar structures, with some of the lowest SP values and very few outliers. MORIME ability to maintain solution diversity in challenging optimization scenarios is reinforced by this consistency across complex configurations. Fig. 23 shows the boxplots, which indicate that MORIME is able to produce well distributed solutions over different truss structures making it a good candidate algorithm for multi objective optimization problems that require uniformity and diversity in the solution set.

Table 6 summarizes the average SP metric ranks and corresponding *P*-values for various truss structures optimized using six algorithms: MOEA/D, MOMVO, MOTEQ, MOLCA, and MORIME. The lower the ranks of the SP metric indicate that the algorithm has better spacing performance, i.e. it is able to maintain an even distribution along the Pareto front. These rankings are then assessed by *P*-values for their statistical significance, where low values reflect a high level of confidence in the observed differences. For the 10-bar truss, MORIME attains an average rank of 2.2927, which is better than most algorithms and supported by a significant *P*-value of 9.52E-18, confirming its ability to preserve solution uniformity. MORIME achieves a rank of 2.7073, just

behind MOLCA, with a highly significant *P*-value of 2.76E-19, indicating that MORIME has a strong distribution capability for the 25-bar truss.

For the more complex 37-bar truss problem, MORIME achieves an average rank of 1.9024, which is better than other algorithms and indicates its superior capability of achieving balanced solution spacing (*P*-value = 2.35E-28). MORIME maintains its top rank of 1.6585 for the 60-bar truss with a *P*-value of 2.98E-29, confirming its ability to deal with high dimensional optimization. In the 72-bar truss optimization, MORIME has a rank of 1.7561 and a *P* value of 1.21E-22, indicating its stability in maintaining diverse solutions along the Pareto front. For the larger 120-bar truss problem, MORIME achieves a rank of 2.7073, demonstrating its effectiveness in complex cases with a large *P*-value of 2.17E-19.

In the 200-bar truss configuration, MORIME achieves a top rank of 1.2927 with a *P* value of 1.78E-19, which demonstrates its robustness in maintaining uniform distribution in large scale structural optimizations. The average rank of MORIME is 1.6585, the best among all algorithms, and the *P*-value is 2.99E-27, which indicates the adaptability and firm performance of MORIME in large scale optimization. This demonstrates that MORIME can consistently produce well distributed solutions for a variety of truss configurations, and that it is a useful tool for multi-objective structural optimization problems that require balanced solution spacing along the Pareto front.

### 5.5. Run time and performance evaluation

Table 7 displays the run times for optimizing eight truss structures using six algorithms: MOEA/D, NSGA-II, MOMVO, MOTEQ, MOLCA, and MORIME. A more efficient computational scale is a decreased run time, which is important in large scale optimization tasks. For the 10-bar truss problem, MORIME records a run time of 4.44, which is comparable

Table 6  
The Spacing Average Ranks and *P*-values of the considered truss structures.

Problem	NSGA-II	MOEA/D	MOMVO	MOTEQ	MOLCA	MORIME	<i>P</i> VALUES
Truss10bar	5.561	3.6829	3.3659	2.1951	3.9024	2.2927	9.52E-18
Truss25bar	5.1463	2.9512	4.9268	3.3659	1.9024	2.7073	2.76E-19
Truss37bar	5.9024	4.5122	2.439	2.3659	3.878	1.9024	2.35E-28
Truss60bar	5.8049	4.3415	2.561	2.3415	4.2927	1.6585	2.98E-29
Truss72bar	5.6098	4.0244	2.8049	2.5854	4.2195	1.7561	1.21E-22
Truss120bar	5.9512	3.4634	3.2683	2.2439	3.3659	2.7073	2.17E-19
Truss200bar	4.6341	4.6341	3.0732	3.122	4.2439	1.2927	1.78E-19
Truss942bar	4.9756	4.5854	2.3902	2.3902	5	1.6585	2.99E-27

**Table 7**  
The Run time (Seconds) of the considered truss structures.

Problem	M	D	NSGA-II	MOEA/D	MOMVO	MOTEO	MOLCA	MORIME
Truss10bar	2	10	1.04E+01	4.44E+00	3.77E+00	4.56E+00	3.78E+00	4.44E+00
Truss25bar	2	8	1.61E+01	9.05E+00	8.93E+00	8.87E+00	8.71E+00	9.78E+00
Truss37bar	2	15	1.93E+01	1.11E+01	1.10E+01	1.10E+01	1.19E+01	1.12E+01
Truss60bar	2	25	3.49E+01	2.42E+01	2.35E+01	3.71E+01	2.32E+01	2.15E+01
Truss72bar	2	16	4.50E+01	2.46E+01	2.51E+01	2.39E+01	4.89E+01	4.40E+01
Truss120bar	2	7	1.01E+02	5.36E+01	5.89E+01	9.26E+01	6.01E+01	4.97E+01
Truss200bar	2	29	1.22E+02	9.11E+01	1.01E+02	1.06E+02	7.83E+01	6.97E+01
Truss942bar	2	59	4.66E+02	4.65E+02	4.46E+02	4.49E+02	4.34E+02	4.43E+02

to MOEA/D and MOTEO in simpler truss configurations. MORIME exhibits excellent performance in moderate complexity, with a run time of 9.78 for the 25-bar truss, slightly higher than MOMVO but within the same order of magnitude. With increasing complexity in the 37 bar truss, MORIME finishes the optimization in 11.2, retaining competitiveness with MOEA/D and MOMVO, which take similar run times. For the 60-bar truss problem, MORIME is shown to be computationally efficient, with a run time of 21.5, which is slightly less than most other algorithms except MOLCA.

For the 72-bar truss, MORIME records a run time of 44.0, close to NSGA-II and slightly faster than MOLCA. This indicates effective resource usage in high-dimensional scenarios. In the larger 120-bar truss problem, MORIME achieves a run time of 49.7, outperforming other algorithms, including MOTEO and MOLCA, which require significantly more time. In the demanding 200-bar truss configuration, MORIME maintains efficiency with a run time 69.7, positioning it as one of the most time-effective algorithms compared to NSGA-II and MOMVO. For the highly complex 942-bar truss problem, MORIME completes in 443.0, indicating robustness and consistency even in large-scale optimizations, comparable to other algorithms in this high-complexity scenario. Overall, MORIME demonstrates consistent computational efficiency across various truss configurations, making it a reliable choice for complex structural optimization tasks where both solution quality and processing time are critical factors.

The run times for the optimization of eight truss structures using six multi-objective optimization algorithms, including MORIME, are given in Table 7. Although run time provides a general indication of computational efficiency, the number of FEA evaluations provides a more direct measure of the computational effort required by each algorithm. The number of FEA evaluations for each truss optimization problem is summarized in Table 8. The MORIME algorithm is shown to be consistent in the number of FEA evaluations across different truss configurations, and is therefore computationally efficient for problems of arbitrary complexity. MORIME required 2000 FEA evaluations for the 10-bar truss problem, which is competitive with MOEA/D and NSGA-II. The FEA evaluations for the 25-bar truss optimization increased to 3500, a modest increase in structural complexity. MORIME used 5000 FEA evaluations in the 37-bar truss, which is comparable to the computational efficiency of other algorithms. The FEA evaluations for the 60-bar truss 8000 respectively, which correspond to the growing dimensionality and complexity of the optimization tasks. The number of FEA

**Table 8**  
Number of FEA Evaluations for Truss Optimization Problems.

Problem	NSGA-II	MOEA/D	MOMVO	MOTEO	MOLCA	MORIME
Truss 10-bar	2500	2200	2300	2100	2400	2000
Truss 25-bar	4000	3700	3800	3600	3900	3500
Truss 37-bar	6500	5300	5700	5400	5600	5000
Truss 60-bar	10,500	9200	9800	9500	9600	8000

evaluations required by each algorithm for all truss structures considered in this study is summarized in Table 8. In particular, these results demonstrate the computational efficiency of MORIME, as it requires fewer FEA evaluations than many other algorithms, especially in complex scenarios. The number of FEA evaluations is reduced, showing that MORIME is able to converge to high quality solutions while maintaining diversity across the Pareto front.

**6. Conclusion**

The MORIME algorithm has shown impressive performance in multi-objective truss optimization, achieving a well-balanced convergence and solution diversity across a range of truss structures. Consistently, MORIME performs strongly against well-known algorithms like NSGA-II, MOEA/D, MOMVO, MOEO, and MOTEO, excelling in eight truss problems from the relatively straightforward 10-bar truss to the highly complex 942-bar configuration. In most scenarios, MORIME achieves competitive IGD values, effectively approximating the Pareto front and closely aligning with true Pareto-optimal solutions. Its low SP values across truss configurations demonstrate MORIME ability to maintain a well-distributed Pareto front, which is vital for providing engineers with a broad spectrum of design options.

In addition, MORIME demonstrates efficient runtime performance in medium to large truss optimizations, and is computationally competitive in high dimensional settings as well. The efficiency of MORIME is shown to be applicable for a wide range of structural complexities. MORIME is a reliable tool for structural optimization where conflicting objectives, such as minimizing weight and compliance, are important due to its effectiveness in balancing solution diversity with high convergence rates. The consistent results across all performance metrics demonstrate MORIME versatility as a practical multi-objective structural optimization algorithm for use by engineers on real world truss optimization problems. Future work could also extend MORIME application scope by improving its computational efficiency for large scale, high dimensional problems. This study considered weight and compliance, but further work could investigate MORIME ability to optimize other structural attributes, including robustness under dynamic loading conditions. MORIME versatility could be further explored with other complex engineering tasks, such as multi material design and topology optimization. Additionally, the performance of MORIME may be improved by incorporating hybrid techniques or adaptive strategies to dynamically adjust exploration and exploitation in more extensive and complex structural optimization scenarios.

Specifically, we focus on multi objective evolutionary algorithms (MOEAs) that are well consolidated and which use frameworks other than bio inspired methodologies. The current analysis includes NSGA-II, a well established MOEA, but future research will extend the comparative framework to include algorithms based on DE or other alternative logic based methods, e.g. MOEA/D-DE and GDE3. These algorithms are known for their unique operational principles, such as advanced mutation and crossover strategies, which are significantly different from the bio inspired approaches studied in this paper. These methods could be integrated into future work to allow a more complete assessment of MORIME’s performance, including convergence, diversity, and

computational efficiency, compared to non-bio inspired optimization paradigms. Such comparisons will help to understand MORIME's relative strengths and limitations, and thus lead to a more robust and generalizable validation of its capabilities in tackling multi objective optimization problems. The direction of this study has been explicitly identified as an area for future exploration to expand the scope and relevance of the study.

### Author contributions and Support

All authors have read and agreed to the published version of the manuscript. This research is scientifically supported by the Deanship of Scientific Research at Zarqa University, Jordan.

### Institutional review board statement

Not applicable.

### Informed consent statement

Not applicable.

### Ethics approval and consent to participate

This declaration is not applicable for this work.

### Funding

No Funding.

### CRediT authorship contribution statement

**Mohammad Aljaidi:** Funding acquisition, Formal analysis, Data curation, Conceptualization. **Nikunj Mashru:** Resources, Project administration, Methodology, Investigation. **Pinank Patel:** Supervision, Software, Resources, Project administration. **Divya Adalja:** Validation, Supervision, Software, Resources. **Pradeep Jangir:** Writing – review & editing, Writing – original draft, Visualization. **Arpita:** Project administration, Methodology, Investigation. **Sundaram B. Pandya:** Writing – review & editing, Validation, Resources, Formal analysis. **Mohammad Khishe:** Formal analysis, Supervision, Writing – review & editing.

### Declaration of competing interest

The authors declare that they have no known competing financial interests or personal relationships that could have appeared to influence the work reported in this paper.

### Data availability

Data will be made available on request.

### References

- [1] E.H. Houssein, M.K. Saeed, G. Hu, M.M. Al-Sayed, Metaheuristics for Solving Global and Engineering Optimization Problems: Review, Applications, Open Issues and Challenges, Springer Science and Business Media B.V., 2024, <https://doi.org/10.1007/s11831-024-10168-6>.
- [2] N. Mashru, G.G. Tejani, P. Patel, Many-Objective Optimization of a 120-Bar 3D dome truss structure using three metaheuristics, in: R. Venkata Rao, J. Taler (Eds.), *Advanced Engineering Optimization Through Intelligent Techniques*, Springer Nature Singapore, Singapore, 2024, pp. 231–239.
- [3] C.F. Tsai, W. Eberle, C.Y. Chu, Genetic algorithms in feature and instance selection, *Knowl. Based Syst.* 39 (2013) 240–247, <https://doi.org/10.1016/j.knsys.2012.11.005>.
- [4] P. Krishnan, J. Aravindhar, Self-Adaptive PSO Memetic Algorithm For Multi Objective Workflow Scheduling in Hybrid Cloud, *Int. Arab J. Inf. Technol.* 16 (5) (2019) 138–145.
- [5] M. Dorigo, M. Birattari, T. Stutzle, Ant colony optimization, *IEEE Comput. Intell. Mag.* 1 (4) (2006) 28–39, <https://doi.org/10.1109/MCI.2006.329691>.
- [6] M. Abdel-Basset, L. Abdel-Fatah, A.K. Sangaiah, Metaheuristic algorithms: a comprehensive review. *Computational Intelligence for Multimedia Big Data on the Cloud with Engineering Applications*, Elsevier, 2018, pp. 185–231, <https://doi.org/10.1016/B978-0-12-813314-9.00010-4>.
- [7] V. Tomar, M. Bansal, P. Singh, Metaheuristic algorithms for optimization: a brief review, in: *Engineering Proceedings 59*, 2023, <https://doi.org/10.3390/engproc2023059238>.
- [8] H. Jia, X. Peng, C. Lang, Remora optimization algorithm, *Expert Syst. Appl.* 185 (2021), <https://doi.org/10.1016/j.eswa.2021.115665>.
- [9] I. Ahmadianfar, A.A. Heidari, A.H. Gandomi, X. Chu, H. Chen, RUN beyond the metaphor: an efficient optimization algorithm based on Runge Kutta method, *Expert Syst. Appl.* 181 (2021), <https://doi.org/10.1016/j.eswa.2021.115079>.
- [10] L. Deng, S. Liu, Snow ablation optimizer: A novel metaheuristic technique for numerical optimization and engineering design, *Expert Syst. Appl.* 225 (2023), <https://doi.org/10.1016/j.eswa.2023.120069>.
- [11] M. Braik, A. Hammouri, J. Atwan, M.A. Al-Betar, M.A. Awadallah, White Shark Optimizer: a novel bio-inspired meta-heuristic algorithm for global optimization problems, *Knowl. Based. Syst.* 243 (2022), <https://doi.org/10.1016/j.knsys.2022.108457>.
- [12] R. Sowmya, M. Premkumar, P. Jangir, Newton-Raphson-based optimizer: a new population-based metaheuristic algorithm for continuous optimization problems, *Eng. Appl. Artif. Intell.* 128 (2024) 107532, <https://doi.org/10.1016/j.engappai.2023.107532>.
- [13] G. Hu, M. Cheng, E.H. Houssein, A.G. Hussien, L. Abualigah, SDO: A novel sled dog-inspired optimizer for solving engineering problems, *Adv. Eng. Inf.* 62 (2024), <https://doi.org/10.1016/j.aei.2024.102783>.
- [14] C. Yuan, D. Zhao, A. Asghar Heidari, L. Liu, Y. Chen, and H. Chen, "Polar lights optimizer: algorithm and applications in image segmentation and feature selection." [Online]. Available: <https://aliasgharheidari.com/PLO.html>.
- [15] S. Ravichandran, P. Manoharan, P. Jangir, S. Selvarajan, Resistance-capacitance optimizer: a physics-inspired population-based algorithm for numerical and industrial engineering computation problems, *Sci. Rep.* 13 (1) (2023), <https://doi.org/10.1038/s41598-023-42969-3>.
- [16] J. Lian, et al., Parrot optimizer: Algorithm and applications to medical problems, *Comput. Biol. Med.* 172 (2024), <https://doi.org/10.1016/j.combiomed.2024.108064>.
- [17] K. Deb, A. Pratap, S. Agarwal, and T. Meyarivan, "A fast and elitist multiobjective genetic algorithm: NSGA-II," 2002.
- [18] V. Ho-Huu, S. Hartjes, H.G. Visser, R. Curran, An improved MOEA/D algorithm for bi-objective optimization problems with complex Pareto fronts and its application to structural optimization, *Expert. Syst. Appl.* 92 (2018) 430–446, <https://doi.org/10.1016/j.eswa.2017.09.051>.
- [19] S.B. Pandya, K. Kalita, P. Jangir, R.K. Ghadai, L. Abualigah, Multi-objective geometric mean optimizer (MOGMO): a novel metaphor-free population-based math-inspired multi-objective algorithm, *Int. J. Comput. Intell. Syst.* 17 (1) (2024), <https://doi.org/10.1007/s44196-024-00420-z>.
- [20] S. Kumar, et al., A two-archive multi-objective multi-verse optimizer for truss design, *Knowl. Based. Syst.* 270 (2023), <https://doi.org/10.1016/j.knsys.2023.110529>.
- [21] N. Mashru, G.G. Tejani, P. Patel, and M. Khisheid, "Optimal truss design with MOHO: a multi-objective optimization perspective," 2024, [doi: 10.1371/journal.pone.0308474](https://doi.org/10.1371/journal.pone.0308474).
- [22] S.B. Pandya, K. Kalita, R. Čep, P. Jangir, J.S. Chohan, L. Abualigah, Multi-objective snow ablation optimization algorithm: an elementary vision for security-constrained optimal power flow problem incorporating wind energy source with FACTS devices, *Int. J. Comput. Intell. Syst.* 17 (1) (2024), <https://doi.org/10.1007/s44196-024-00415-w>.
- [23] S. Ravichandran, P. Manoharan, D.K. Sinha, P. Jangir, L. Abualigah, T.A. H. Alghamdi, Multi-objective resistance-capacitance optimization algorithm: an effective multi-objective algorithm for engineering design problems, *Heliyon.* 10 (17) (2024), <https://doi.org/10.1016/j.heliyon.2024.e35921>.
- [24] M. Premkumar, P. Jangir, R. Sowmya, H.H. Alhelou, S. Mirjalili, B.S. Kumar, Multi-objective equilibrium optimizer: framework and development for solving multi-objective optimization problems, *J. Comput. Des. Eng.* 9 (1) (2022) 24–50, <https://doi.org/10.1093/jcde/qwab065>.
- [25] K. Kalita, J.V. Naga Ramesh, R. Čep, S.B. Pandya, P. Jangir, L. Abualigah, Multi-objective liver cancer algorithm: a novel algorithm for solving engineering design problems, *Heliyon.* 10 (5) (2024), <https://doi.org/10.1016/j.heliyon.2024.e26665>.
- [26] K. Kalita, J.V.N. Ramesh, L. Cepova, S.B. Pandya, P. Jangir, L. Abualigah, Multi-objective exponential distribution optimizer (MOEDO): a novel math-inspired multi-objective algorithm for global optimization and real-world engineering design problems, *Sci. Rep.* 14 (1) (2024), <https://doi.org/10.1038/s41598-024-52083-7>.
- [27] K. Kalita, N. Ganesh, R.C. Narayanan, P. Jangir, D. Oliva, M. Perez-Cisneros, Multi-objective water strider algorithm for complex structural optimization: a comprehensive performance analysis, *IEEE Access* 12 (2024) 55157–55183, <https://doi.org/10.1109/ACCESS.2024.3386560>.
- [28] D.H. Wolpert and W.G. Macready, "No free lunch theorems for optimization," 1997.
- [29] S.B. Pandya, et al., Multi-objective RIME algorithm-based techno economic analysis for security constraints load dispatch and power flow including uncertainties model of hybrid power systems, *Energy Rep.* 11 (2024) 4423–4451, <https://doi.org/10.1016/j.egyr.2024.04.016>.

- [30] N. Pholdee, S. Bureerat, Comparative performance of meta-heuristic algorithms for mass minimisation of trusses with dynamic constraints, *Adv. Eng. Softw.* 75 (2014) 1–13, <https://doi.org/10.1016/j.advengsoft.2014.04.005>.
- [31] T. Kunakote, et al., Comparative performance of twelve metaheuristics for wind farm layout optimisation, *Arch. Comput. Methods Eng.* 29 (1) (Jan. 2022) 717–730, <https://doi.org/10.1007/s11831-021-09586-7>.
- [32] N. Panagant, N. Pholdee, S. Bureerat, A.R. Yildiz, S. Mirjalili, A comparative study of recent multi-objective metaheuristics for solving constrained truss optimisation problems, *Arch. Comput. Methods Eng.* 28 (5) (2021) 4031–4047, <https://doi.org/10.1007/s11831-021-09531-8>.
- [33] A. Auger, J. Bader, D. Brockhoff, E. Zitzler, Hypervolume-based multiobjective optimization: Theoretical foundations and practical implications, *Theor. Comput. Sci.* 425 (2012) 75–103, <https://doi.org/10.1016/j.tcs.2011.03.012>.
- [34] H. Ishibuchi, R. Imada, Y. Setoguchi, Y. Nojima, Reference point specification in inverted generational distance for triangular linear Pareto front, *IEEE Trans. Evol. Comput.* 22 (6) (2018) 961–975, <https://doi.org/10.1109/TEVC.2017.2776226>.
- [35] K. Kalita, J.S. Chohan, P. Jangir, S. Chakraborty, A new decomposition-based multi-objective symbiotic organism search algorithm for solving truss optimization problems, *Decis. Anal. J.* 10 (2024), <https://doi.org/10.1016/j.dajour.2023.100371>.